Journal of Nonlinear Science (2024) 34:78
https://doi.org/10.1007/s00332-024-10058-y

Oscillatory Motions of Multiple Spikes in Three-Component Reaction–Diffusion Systems

Shuangquan Xie[1] · Wen Yang[2] · Jiaojiao Zhang[3,4]

Received: 2 September 2023 / Accepted: 10 June 2024

Abstract

For three specific singular perturbed three-component reaction–diffusion systems that admit N-spike solutions in one of the components on a finite domain, we present a detailed analysis for the dynamics of temporal oscillations in the spike positions. The onset of these oscillations is induced by N Hopf bifurcations with respect to the translation modes that are excited nearly simultaneously. To understand the dynamics of N spikes in the vicinity of Hopf bifurcations, we combine the center manifold reduction and the matched asymptotic method to derive a set of ordinary differential equations (ODEs) of dimension $2N$ describing the spikes' locations and velocities, which can be recognized as normal forms of multiple Hopf bifurcations. The reduced ODE system then is represented in the form of linear oscillators with weakly nonlinear damping. By applying the multiple-time method, the leading order of the oscillation amplitudes is further characterized by an N-dimensional ODE system of the Stuart–Landau type. Although the leading order dynamics of these three systems are different, they have the same form after a suitable transformation. On the basis of the reduced systems for the oscillation amplitudes, we prove that there are at most $\lfloor N/2 \rfloor + 1$ stable equilibria, corresponding to $\lfloor N/2 \rfloor + 1$ types of different oscillations. This resolves an open problem proposed by Xie et al. (Nonlinearity 34(8):5708–5743, 2021) for a

Communicated by Michael Ward.

✉ Shuangquan Xie
xieshuangquan2013@gmail.com

Wen Yang
wenyang@um.edu.mo

Jiaojiao Zhang
zhangjiaojiao@apm.ac.cn

1 School of Mathematics, Hunan University, Changsha 410082, People's Republic of China

2 Department of Mathematics, Faculty of Science and Technology, University of Macau, Taipa, Macau, People's Republic of China

3 University of Chinese Academy of Sciences, Beijing 100049, People's Republic of China

4 Wuhan Institute of Physics and Mathematics, Innovation Academy for Precision Measurement Science and Technology, Chinese Academy of Sciences, Wuhan 430071, People's Republic of China

Published online: 28 June 2024

three-component Schnakenberg system and generalizes the results to two other classic systems. Numerical simulations are presented to verify the analytic results.

Keywords Multiple Hopf bifurcations · Coexistence of multiple oscillatory moving spikes · Matched asymptotic methods · Reduction methods · Three-component reaction–diffusion systems

Mathematics Subject Classification 37L10 · 35K57 · 35B25 · 35B36

1 Introduction

Spatially localized patterns have been observed in diverse physical and chemical experiments (see the survey Vanag and Epstein (2007)). The modeling of these experiments often generates nonlinear reaction–diffusion (RD) systems that admit spatial inhomogeneous solutions localized in small regions. As prototyping models to produce well-localized solutions, several well-known two-component RD systems, such as the Gierer–Meinhardt model (Gierer and Meinhardt 1972), the Gray–Scott model (Pearson 1993) and the Schnakenberg model (Schnakenberg 1979) have been extensively studied. In the large diffusivity ratio limit, these systems can exhibit multiple-spike solutions in the component with a slow diffusion rate. Such spiky patterns have been shown to exhibit various types of instabilities and dynamic behaviors such as spike splitting, temporal oscillations in the spike heights, spike annihilation, and slowly moving spike, see Doelman et al. (2001a, b); Iron et al. (2001); Iron and Ward (2002); Gomez et al. (2021); Ward and Wei (2003a, b) and the book (Wei and Winter 2013) for the Gierer–Meinhardt system, Doelman et al. (2002, 1997); Kolokolnikov et al. (2005a, b); Gomez et al. (2020); Kolokolnikov et al. (2006) for the Gray–Scott system, Iron et al. (2004); Ward and Wei (2002); Gomez et al. (2020) for the Schnakenberg system.

An intriguing phenomenon is the emergence of oscillatory patterns due to the Hopf bifurcation (HB). Typically, increasing the reaction ratio constant of the inhibitor or substrate can lead to a destabilization of the stationary spike solution through the HB. Two distinct types of HB have been examined in the literature: One is associated with “small eigenvalues" that approach zero when the diffusion rate of the activator vanishes; the other is associated with “large eigenvalues" that remain to be constant as the diffusion rate of the activator diminishes. As a reaction-time parameter is increased, either a large eigenvalue or a small eigenvalue will be the first to have a positive real part. If a large eigenvalue crosses the imaginary axis first, oscillations in the spike height occur first. Alternatively, oscillations in the spike position take precedence. For the classic activator-inhibitor Gierer–Meinhardt model, the HB is subcritical and generates unstable time-periodic patterns with spikes oscillating in their heights (Ward and Wei 2003a; Gomez et al. 2021; Kolokolnikov et al. 2021; Veerman 2015). For the activator-substrate systems such as the Gray–Scott model and the Schnakenberg model, the HB for temporal spike height oscillations occurs first and is subcritical at a low feeding rate (Gomez et al. 2020; Kolokolnikov et al. 2021). At a high feeding rate, the HB for temporal spike position oscillations occurs first and is supercritical (Chen and Ward 2009; Xie and Kolokolnikov 2017; Kolokolnikov et al. 2005a; Chen and Ward 2011). It is worth noting that the oscillation in the spike position typically requires both components in the system to be strongly coupled near the spike centers, namely, both the activator and the substrate are localized. One may ask whether it is possible to find stable oscillatory spikes in the positions with the substrate (inhibitor) weakly coupled with the activator. As far as the authors are aware, this appears to be unrealistic for two-component systems. On the other hand, theoretical results obtained for a class of three-component reaction–diffusion equations in Or-Guil et al. (1998) suggest that it is always feasible to find parameters that lead to the propagation of any stationary structure that can be found in the corresponding two-component system. Further studies on three-component systems (Bastiaansen and Doelman 2019; Chirilus-Bruckner et al. 2019) have revealed that localized solutions can exhibit remarkably richer dynamics. This motivates us to consider three-component extensions of some classic two-component models. Recently, a three-component extension of the Schnakenberg model was analyzed in Xie et al. (2021), exhibiting new, previously unobserved behavior: numerical simulations reveal the coexistence of both in-phase and out-of-phase oscillations in the spike positions for a two-spike solution. An open problem proposed there is: *How many stable small-amplitude oscillatory moving patterns can we find for an N-spike solution when N translation modes are excited?* One goal of this paper is to address this problem.

In this paper, we consider three-component extensions of three singularly perturbed two-component systems

$$\begin{cases} u_t = \varepsilon^2 u_{xx} + f(u, v) - \kappa w, \\ 0 = D v_{xx} + g(u, v), \qquad\qquad x \in (-1, 1), \quad t \geq 0, \\ \tau w_t = u - w, \\ \text{Neumann boundary conditions for at } x = \pm 1. \end{cases} \tag{1.1}$$

in the limit

$$\varepsilon \ll 1. \tag{1.2}$$

The first system is the nondimensional Gierer–Meinhardt model with reaction terms as

$$f(u, v) = -(1-\kappa)u + u^2/v, \quad g(u, v) = -v + \varepsilon^{-1}u^2. \tag{1.3}$$

The second system is the nondimensional Gray–Scott model at a low feeding rate with

$$f(u, v) = -(1-\kappa)u + Au^2 v, \quad g(u, v) = 1 - v - \varepsilon^{-1}u^2 v. \tag{1.4}$$

The third system is the nondimensional Schnakenberg model at a low feeding rate with

$$f(u, v) = -(1-\kappa)u + u^2 v, \quad g(u, v) = \frac{1}{2} - \varepsilon^{-1}u^2 v. \tag{1.5}$$

The coupling coefficient κ is independent of ε and assumed to be $0 < \kappa < 1$. The nondimensionalization details of the Gierer–Meinhardt system are provided in Appendix B. The third component w acts as an inhibitor to the first one, whose kinetic is motivated by the FitzHugh-Nagumo system. In the chemical system, it could symbolize a substance produced as a byproduct of the activator's production, which in turn has a negative effect on the activator, representing a depletion of resources or accumulation of waste that inhibits the reaction. These three RD systems degenerate to their corresponding standard two-component systems when $\tau = 0$, which have the following two properties when $\varepsilon \ll 1$:

- When D satisfies some explicit constraints, there exists a stable solution consisting of N evenly distributed spikes with equal height.
- For a stable N-spike solution, the first N leading eigenvalues are negative real and $\mathcal{O}(\varepsilon^2)$, whose associated eigenmodes are translation modes in the leading order.

See Iron et al. (2001); Kolokolnikov et al. (2006); Iron et al. (2004) for related results on each model. Setting $\tau > 0$ does not change the equilibrium state but has an impact on the stability. Hence the existence of symmetric N-spike steady-state solutions centered at $x_k = -1 + \frac{2j-1}{N}$, $j = 1, \ldots, N$ to the system (1.1) is readily established. In Or-Guil et al. (1998), the authors have shown that the eigenvalues that determine the stability of an equilibrium state in the extended systems (1.1) for general f and g can be explicitly determined by the eigenvalues of their two-component counterparts, suggesting that we can obtain some analytic results if we know the solution explicitly. For the systems under consideration, the first N leading eigenvalues are negative real and of the order ε^2, allowing us to find N thresholds located within a region of width $\mathcal{O}(\varepsilon^2)$. These thresholds are identical in the limit $\varepsilon \to 0$, and N pairs of complex-conjugated eigenvalues pass through the imaginary axis as τ exceeds the critical value τ_c, which then excite the corresponding translation modes and initiate the multiple types of oscillations in the spike positions. We aim to understand the stable small-amplitude oscillatory patterns we can finally observe.

Figure 1 illustrates the aforementioned phenomenon in the Schnakenberg model. For five spikes, there are five eigenvalues that cross the imaginary axis for τ slightly exceeding $\frac{1}{\kappa}$, which causes the spike center to oscillate periodically. The long-time dynamics settle into one of three possible stable oscillatory patterns, corresponding to the three stable equilibria in the amplitude equations. Which pattern is chosen depends on the initial conditions. For six spikes, there are six eigenvalues that cross the imaginary axis for values of τ well beyond $1/\kappa$. The long-time dynamics settle into one of four possible oscillatory stable patterns, corresponding to the four stable equilibria in the amplitude equations. Four types of oscillations coexist for the same parameter values, and the pattern selection mechanism depends only on the initial conditions.

With the goal to delineate the manifestation of periodically moving patterns, we perform a detailed study of temporal oscillations in the spike positions near Hopf bifurcations for N-spike solutions in three singular perturbed RD systems. In particular, we demonstrate that N Hopf modes become unstable when τ passes $\frac{1}{\kappa}$ in the limit $\varepsilon \to 0$, leading to multiple types of oscillations at the onset of instability, which then saturate into a particular stable periodic orbit. Next, we perform a multiple-scale perturbation expansion in the vicinity of the bifurcation point and derive a set of ODE equations, explicitly describing the dynamics of multiple spikes. Finally, based on the

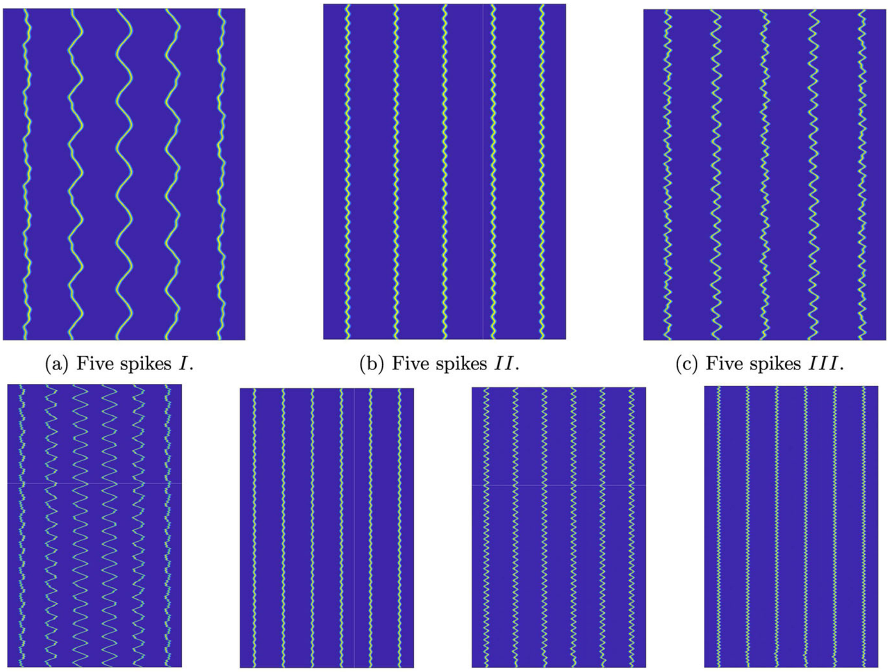

(a) Five spikes I. (b) Five spikes II. (c) Five spikes III.

(d) Six spikes I. (e) Six spikes II. (f) Six spikes III. (g) Six spikes IV.

Fig. 1 Space-time plots of the activator distribution u for different initial N-spike configurations obtained from numerically solving the system (1.1) using FlexPDE7 (Inc 2020) with Schnakenberg type of nonlinearities in Eq. (1.5). The horizontal axis is space, and the vertical axis is time. The parameters are $\varepsilon = 0.005,\ \kappa = 0.8,\ D = \frac{1}{24N^3}$ for $N = 5, 6$. (a-c) three different final states of oscillatory five spikes at $\tau = 1.01/\kappa$. The only difference between them is the initial perturbation we select. (d-g) four different final states of oscillatory five spikes at $\tau = 1.015/\kappa$. The only difference between them is the initial perturbation we select

reduced description, we prove that the leading order oscillations settle into one of the $\lfloor N/2 \rfloor + 1$ possible stable states.

The contribution of this paper is twofold. First, we extend the results in Xie et al. (2021) to another two classic RD systems, showing that the coexistence of multiple oscillation patterns is a universal phenomenon. Second, we resolve the open problem raised in Xie et al. (2021), giving a complete classification of the stable oscillation pattern slightly beyond multiple Hopf bifurcations.

The outline of this paper is as follows. In §2, we derive the relation between the eigenvalues of three-component systems and their associated two-component systems. We show that an N-spike solution undergoes a transition from a stationary state to an oscillatory state as the parameter τ is increased past some threshold τ_c; this instability is triggered via a Hopf bifurcation of drift type. Moreover, N small eigenvalues (controlling the motion of N spikes) undergo Hopf bifurcations nearly simultaneously. Consequently, a complex interaction between the different modes can occur, leading to the coexistence of multiple possible oscillating patterns. A key open problem then is determining whether these time-periodic solutions bifurcating from the N-spike stationary solution are stable.

In §3, we formally derive a reduced description of spike positions and velocities to unfold the dynamics near the bifurcation point for the Gierer–Meinhardt model, which is essentially the Hopf normal form. In general, this can be done by following the weakly nonlinear analysis developed in Veerman (2015) or similar approaches used in Gurevich et al. (2006). However, the leading eigenmode in these references is associated with an $\mathcal{O}(1)$ eigenvalue, in contrast with $\mathcal{O}(\varepsilon^2)$ eigenvalue in this article. Moreover, only one Hopf mode is assumed to be excited in Veerman (2015) and Gurevich et al. (2006), while we study the scenario when multiple Hopf modes are excited. These differences make our problem more delicate and require intricate analysis in a hierarchy of problems in each order of ε. We will use a combination of the matched asymptotic methods and the center manifold reduction to reduce the PDE system to a set of ODE systems up to $\mathcal{O}(\varepsilon^2)$. We then apply the multiple-scale method to obtain a leading order approximation of the solution to the reduced system, revealing that the spikes oscillations consist of different oscillating modes in the leading order of ε, whose amplitudes are subject to a system of ordinary differential equations that can be seen as the Landau equations. Each equilibrium point of the amplitude equations corresponds to an oscillatory state, the stability of which determines the final state we can observe numerically.

In §4, we classify the equilibria of the amplitude equations with respect to τ and rigorously prove that the Landau equations have at most 2^N non-negative equilibria, among which $\lfloor N/2\rfloor + 1$ are stable, suggesting that at most $\lfloor N/2\rfloor + 1$ stable small-amplitude oscillatory pattern can be observed in the leading order. Finally, in §5 we summarize our results and highlight some open problems for future research.

2 Hopf Bifurcations

In this section, we investigate the bifurcations induced by increasing the reaction ratio τ for general three-component systems (1.1). The analysis for the extended Schnakenberg model has been carried out in Xie et al. (2021). Here we sketch the analysis for a general system. We consider the dynamics linearized around the stationary solution (u_s, v_s, u_s) and compare it with the dynamics in the special case $\tau = 0$.

We define the linear operator $\mathcal{L}_0$ as follows:

$$\mathcal{L}_0 := \begin{pmatrix} \varepsilon^2\Delta + f_u(u_s, v_s) - \kappa & f_v(u_s, v_s) \\ g_u(u_s, v_s) & D\Delta + g_v(u_s, v_s) \end{pmatrix}. \tag{2.1}$$

For a perturbation $[\phi_\tau, \psi_\tau, \eta_\tau] \ll 1$ to the steady state $[u_s, v_s, u_s]$, we obtain the following eigenvalue problem for $\tau = 0$:

$$\gamma\phi_0 = \varepsilon^2\Delta\phi_0 + f_u(u_s, v_s)\phi_0 + f_v(u_s, v_s)\psi_0 - \kappa\eta_0, \tag{2.2a}$$
$$0 = D\Delta\psi_0 + g_u(u_s, v_s)\phi_0 + g_v(u_s, v_s)\psi_0, \tag{2.2b}$$
$$0 = \phi_0 - \eta_0; \tag{2.2c}$$

and for $\tau \neq 0$:

$$\lambda\phi_\tau = \varepsilon^2\Delta\phi_\tau + f_u(u_s, v_s)\phi_\tau + f_v(u_s, v_s)\psi_\tau - \kappa\eta_\tau, \tag{2.3a}$$

$$0 = D\Delta\psi_\tau + g_u(u_s, v_s)\phi_\tau + g_v(u_s, v_s)\psi_\tau, \tag{2.3b}$$

$$\tau\lambda\eta_\tau = \phi_\tau - \eta_\tau, \tag{2.3c}$$

where we denote the eigenvalues of the three-component system at $\tau = 0$ as γ and the eigenvalues at $\tau \neq 0$ as λ. The system Eq. (2.2) can be rewritten as

$$\gamma \begin{pmatrix} \phi_0 \\ 0 \end{pmatrix} = \mathcal{L}_0 \begin{pmatrix} \phi_0 \\ \psi_0 \end{pmatrix}, \tag{2.4}$$

Note that the third row of system Eq. (2.3) is a linear algebraic equation. We solve η_τ w.r.t ϕ_τ to obtain

$$\eta_\tau = \frac{1}{1+\tau\lambda}\phi_\tau. \tag{2.5}$$

Using this to remove η_τ in other two rows, we obtain

$$\lambda\left(1 - \frac{\kappa\tau}{1+\tau\lambda}\right)\begin{pmatrix} \phi_\tau \\ 0 \end{pmatrix} = \mathcal{L}_0 \begin{pmatrix} \phi_\tau \\ \psi_\tau \end{pmatrix}. \tag{2.6}$$

Comparing Eq. (2.4) and Eq. (2.6), we compute λ and $[\phi_\tau, \psi_\tau, \eta_\tau]$ based on γ and $[\phi_0, \psi_0]$ as follows:

$$\lambda = \frac{\tau(\kappa+\gamma)-1}{2\tau} \pm \sqrt{\frac{\gamma}{\tau} + \left(\frac{\tau(\kappa+\gamma)-1}{2\tau}\right)^2}, \tag{2.7a}$$

$$[\phi_\tau, \psi_\tau, \eta_\tau] = [\phi_0, \psi_0, \frac{1}{1+\tau\lambda}\phi_0]. \tag{2.7b}$$

Equation (2.7) implies that the eigenvalue and eigenvector at $\tau \neq 0$ can be directly obtained from those at $\tau = 0$. When τ is increased, the bifurcations detected are ranked according to the value of the related γ. Thus, if an N-spike solution is stable for $\tau = 0$, this solution will stay stable until τ is increased up to $\frac{1}{\kappa+\gamma_{\max}}$.

We are interested in the stability of an N-spike solution and the dynamics of N spikes in the vicinity of the bifurcation. Denote the u component of an N-spike quasi-equilibrium solution as

$$u_s \sim \sum_{k=1}^{N} u_c\left(\frac{x - x_k}{\varepsilon}\right), \tag{2.8}$$

where x_k is the equilibrium position, $\{x_k = -1 + \frac{2k-1}{N},\ k = 1, \ldots, N\}$. For the systems we consider in this paper, the first N leading eigenvalues $\{\gamma_k,\ k = 1, \ldots, N\}$ are negative real and of the order ε^2 (see the computations in Iron et al. (2001); Kolokolnikov et al. (2006); Iron et al. (2004)). Hence, increasing the bifurcation parameter τ to pass $\tau_k := \frac{1}{\kappa+\gamma_k}$ pushes the k-th eigenvalue to cross the imaginary axis with pure imaginary numbers. Since the eigenvector corresponding to γ_k is a translation mode that can be written as a linear combination of $\left\{u_c'\left(\frac{x-x_k}{\varepsilon}\right), k=1,\dots N\right\}$, N translation modes are destabilized when $\tau > \tau_N$, leading to complex motions in the spike positions. In the limit $\varepsilon \ll 1$, we have $\tau_k \sim \frac{1}{\kappa}$ for $k=1,\cdots,N$, then N Hopf modes become excited almost simultaneously when τ is above $\tau_c := \frac{1}{\kappa}$.

Now we give a rough description of the dynamics near the bifurcation point. We denote the ϕ component of corresponding first N eigenvectors as

$$\phi_{0,k} \sim \sum_{j=1}^{N} Q_{j,k} u_c'\left(\frac{x-x_j}{\varepsilon}\right), \; k=1,\dots,N, \tag{2.9}$$

where $Q_{j,k}$ are constants determining the moving direction of j-th spike under the influence of k-th mode $\phi_{0,k}$. We define Q as the matrix with $Q_{j,k}$ as its entries,

$$Q := \{Q_{j,k}\} = \left(\mathbf{q}_1, \cdots, \mathbf{q}_N\right). \tag{2.10}$$

For the Schnakenberg model, the Gierer–Meinhardt model and the Gray–Scot model, they have the same Q (see Iron et al. (2001); Kolokolnikov et al. (2006); Iron et al. (2004)) that can be computed as

$$\mathbf{q}_N = \sqrt{\frac{1}{N}}[1,-1,1,\cdots,(-1)^{N+1}]^{\mathsf{T}}, \tag{2.11a}$$

$$\mathbf{q}_k = [Q_{1,k},\cdots,Q_{N,k}]^T, \quad k=1,\cdots,N-1, \tag{2.11b}$$

$$Q_{j,k} = \sqrt{\frac{2}{N}}\sin\left(\frac{\pi k}{N}(j-\frac{1}{2})\right). \tag{2.11c}$$

Here $[\;\cdot\;]^{\mathsf{T}}$ denotes the transpose. If we increase the control parameter τ slightly beyond τ_c as $\tau = \tau_c + \varepsilon^2\hat{\tau}$, these N translation modes dominate the dynamics. Then the dynamics can be approximated by

$$u \sim \sum_{k=1}^{N} u_c\left(\frac{x-x_k}{\varepsilon}\right) + \sum_{k=1}^{N}\left(A_k e^{\lambda_k t}\phi_{0,k} + \text{c.c.}\right), \tag{2.12}$$

where A_k are constant oscillation amplitudes and c.c. is referred to as the complex conjugate. Substituting $\tau = \tau_c + \varepsilon^2\hat{\tau}$ into Eq. (2.7), we obtain

$$\lambda_k = \frac{\hat{\tau}(\kappa+\gamma_k)\varepsilon^2 + \gamma_k/\kappa}{2(1/\kappa+\varepsilon^2\hat{\tau})} + \sqrt{\frac{\gamma_k}{(1/\kappa+\varepsilon^2\hat{\tau})} + \left(\frac{\hat{\tau}(\kappa+\gamma_k)\varepsilon^2 + \gamma_k/\kappa}{2(1/\kappa+\varepsilon^2\hat{\tau})}\right)^2}, \quad k=1,\dots,N. \tag{2.13}$$

Note that $\gamma_k \sim \mathcal{O}(\varepsilon^2),\; k=1,\dots,N$. Let $\mu_k = \frac{\hat{\tau}\kappa^2+\gamma_k\varepsilon^{-2}}{2}$ and $\omega_k = \sqrt{-\kappa\gamma_k\varepsilon^{-2}}$, we can rewrite λ_k as

$$\lambda_k = \varepsilon^2\mu_k + \mathcal{O}(\varepsilon^3) + i\left(\varepsilon\omega_k + \mathcal{O}(\varepsilon^2)\right), \tag{2.14}$$

then the corresponding factor $e^{\lambda_k t}$ in Eq. (2.12) can be decomposed into the oscillatory factor $e^{i\varepsilon\omega_k t}$ and the growth factor $e^{\varepsilon^2\mu_k t}$. This suggests that the amplitudes and phases change at different time scales. Using (2.9) and taking the leading order part of λ_k, we rewrite Eq. (2.12) as

$$\begin{aligned} u &\sim \sum_{k=1}^{N} u_c\left(\frac{x-x_k}{\varepsilon}\right) + \sum_{k=1}^{N}\left(A_k e^{i\varepsilon\omega_k t}\phi_{0,k} + c.c\right) \\ &\sim \sum_{k=1}^{N} u_c\left(\frac{x-x_k}{\varepsilon}\right) + \sum_{k=1}^{N}\left(A_k e^{i\varepsilon\omega_k t} + c.c\right)\sum_{j=1}^{N} Q_{j,k} u_c'\left(\frac{x-x_j}{\varepsilon}\right) \\ &\sim \sum_{k=1}^{N}\left(u_c\left(\frac{x-x_k}{\varepsilon}\right) - u_c'\left(\frac{x-x_k}{\varepsilon}\right)\sum_{j=1}^{N} Q_{k,j} B_j \cos\left(\varepsilon\omega_j t + \theta_j\right)\right) \\ &\sim \sum_{k=1}^{N} u_c\left(\frac{x-x_k-\varepsilon p_k}{\varepsilon}\right), \end{aligned} \tag{2.15}$$

where $A_j = -\frac{1}{2}B_j e^{i\theta_j}$, $p_k = \sum_{j=1}^{N} Q_{k,j} B_j \cos(\varepsilon\omega_j t + \theta_j)$. We point out that $B_j = 2|A_j|$ and θ_j evolves at a much slower time scale, namely $\varepsilon^2 t$, and requires a higher order analysis.

It is worth noting that there is a correction term to w we must include in the higher order analysis according to (2.7b). Expanding (2.7b), we obtain

$$\begin{pmatrix} \phi_{0,k} \\ \psi_{0,k} \\ \frac{1}{1+\tau\lambda_k}\phi_{0,k} \end{pmatrix} \sim \begin{pmatrix} \phi_{0,k} \\ \psi_{0,k} \\ \phi_{0,k} \end{pmatrix} - i\tau_c\varepsilon\omega_k \begin{pmatrix} 0 \\ 0 \\ \phi_{0,k} \end{pmatrix}, \quad k = 1, \ldots, N. \tag{2.16}$$

The term $[0, 0, \phi_{0,k}]^T$ is extracted separately in the expansion (3.5).

The ODE system describing the dynamics of B_j for the Schnakenberg model has been derived in Xie et al. (2021), where the method of matched asymptotic analysis and the method of multiple scales are utilized. Our goal in the next section is to write down the ordinary differential equation of the amplitude B_j for the other two systems.

3 Slow Dynamics Close to the Hopf Bifurcation

In this section, we investigate the dynamics in the vicinity of N-fold Hopf bifurcations by projecting the dynamics into the space expanded by N excited translation modes. As the eigenvalues have a different scaling in real and imaginary part when $\tau = \frac{1}{\kappa} + \hat{\tau}\varepsilon^2$, the analysis involves different orders of ε. We will derive the dynamics by a combination of the matched asymptotic methods and the center manifold reduction. The derivation has been done for the Schnakenberg model in Xie et al. (2021), we take the same strategy to derive the reduced dynamics for the Gierer–Meinhardt model. As to the Gray–Scott model, we omit the derivation and only present the results.

3.1 Reduced ODE System for the Gierer–Meinhardt Model

We consider the extended Gierer–Meinhardt system:

$$\begin{cases} u_t = \varepsilon^2 u_{xx} - (1-\kappa)u + u^2/v - \kappa w, \\ 0 = Dv_{xx} - v + u^2/\varepsilon, \\ \tau w_t = u - w, \\ \text{Neumann boundary conditions at } x = \pm 1. \end{cases} \tag{3.1}$$

For a initial condition with N spikes located at positions close to their equilibrium positions, the spikes will start to oscillate with a small amplitude when τ slightly exceeds $\frac{1}{\kappa}$; thus we assume the k-th spike to be located at $\hat{x}_k = x_k + \varepsilon p_k$ according to Eq. (2.15). Then, we calculate the solution in the inner region near the k-th spike where $|x - \hat{x}_k| \sim \mathcal{O}(\varepsilon)$, and in the outer region away from the k-th spike where $|x - \hat{x}_k| \sim \mathcal{O}(1)$. The equations for the position of each spike are determined by matching the outer and inner solutions.

Inner region: Near the k-th spike, we introduce variable $y = \frac{x - x_k - \varepsilon p_k(t)}{\varepsilon}$, and rewrite u, v and w as

$$u(x,t) = U(y,t), \quad v(x,t) = V(y,t), \quad w(x,t) = W(y,t). \tag{3.2}$$

Then, the system (3.1) becomes

$$-U_y \dot{p}_k + \frac{\partial U}{\partial t} = U_{yy} - (1-\kappa)U + U^2/V - \kappa W, \tag{3.3a}$$

$$0 = DV_{yy} - \varepsilon^2 V + \varepsilon U^2, \tag{3.3b}$$

$$(\frac{1}{\kappa} + \varepsilon^2 \hat{\tau}) \left(-W_y \dot{p}_k + \frac{\partial W}{\partial t} \right) = U - W. \tag{3.3c}$$

The far-field conditions as $|y| \to \infty$ are that U and W tend to zero exponentially, whereas the conditions for V contain some constants that must be determined by matching with the outer solution.

To facilitate the analysis, we introduce slow time scales

$$T_1 = \varepsilon t, \; T_2 = \varepsilon^2 t, \cdots,$$

so that

$$\dot{p}_k = \varepsilon \frac{\partial p_k}{\partial T_1} + \varepsilon^2 \frac{\partial p_k}{\partial T_2} + \cdots, \tag{3.4}$$

and use the following expansion in the spirit of center manifold reduction according to Eqs. (2.15) and (2.16)

$$\begin{bmatrix} U \\ V \\ W \end{bmatrix} = \begin{bmatrix} U_0 \\ V_0 \\ W_0 \end{bmatrix} + \varepsilon \left(\begin{bmatrix} U_1 \\ V_1 \\ W_1 \end{bmatrix} + \alpha_k \begin{bmatrix} 0 \\ 0 \\ U_{0y} \end{bmatrix} \right) + \varepsilon^2 \begin{bmatrix} U_2 \\ V_2 \\ W_2 \end{bmatrix} + \varepsilon^3 \begin{bmatrix} U_3 \\ V_3 \\ W_3 \end{bmatrix} + h.o.t, \tag{3.5}$$

with $[U_0, V_0, W_0]$ being the spike profile and $[U_k, V_k, W_k]$ being orthogonal to $[U_{0y}, V_{0y}, U_{0y}]$ and $[0, 0, U_{0y}]$ for $k \geq 1$. Note that $[U_{0y}, V_{0y}, U_{0y}]$ has been implicitly included into $[U_0, V_0, U_0]$ in the way of Eq. (2.15) and $\alpha_k[0, 0, U_{0y}]$ accounts for the corrections from Eq. (2.16). We remark that $[U_{0y}, V_{0y}, U_{0y}]$ and $[0, 0, U_{0y}]$ are the basis of the center manifold near the spike center. Thus we require the rest terms to be orthogonal to them. Substituting Eq. (3.5) and Eq. (3.4) into Eq. (3.3) and collecting different terms in order of ε, we obtain a hierarchy of equations.

In the leading order, we obtain

$$0 = U_{0yy} - (1-\kappa)U_0 + U_0^2/V_0 - \kappa W_0, \tag{3.6a}$$
$$0 = DV_{0yy}, \tag{3.6b}$$
$$0 = U_0 - W_0. \tag{3.6c}$$

The conditions needed to match to the outer solution are that V_0 is bounded and $U_0, W_0 \to 0$ as $|y| \to \infty$. Thus, the solution to Eq. (3.6) is

$$U_0 = c_{k,0}\rho(y), \;\; V_0 = c_{k,0}, \;\; W_0 = c_{k,0}\rho(y), \tag{3.7}$$

where $c_{k,0}$ are constants we will determine by matching and $\rho(y) = \frac{3}{2}\mathrm{sech}^2(\frac{y}{2})$ satisfying

$$\rho'' - \rho + \rho^2 = 0; \quad \rho \to 0 \text{ as } |y| \to \infty; \quad \rho'(0) = 0. \tag{3.8}$$

Since V_0 is a constant, the orthogonality conditions are simplified to be

$$\langle U_k, U_{0y}\rangle = 0, \quad \langle W_k, U_{0y}\rangle = 0, \text{ for } k \geq 1 \tag{3.9}$$

where $\langle f, g\rangle$ denotes the inner product of two functions over $\mathbb{R}$,

$$\langle f, g\rangle := \int_{-\infty}^{\infty} f(y)g(y)\,\mathrm{d}y. \tag{3.10}$$

In the order of ε, we obtain

$$-U_{0y}\frac{\partial p_k}{\partial T_1} - \mathcal{F}_1 = U_{1yy} - (1-\kappa)U_1 + 2U_0U_1/V_0 - \kappa(W_1 + \alpha_k U_{0y}), \tag{3.11a}$$
$$0 = DV_{1yy} + U_0^2, \tag{3.11b}$$
$$-W_{0y}\frac{\partial p_k}{\partial T_1} = \kappa\left(U_1 - (W_1 + \alpha_k U_{0y})\right), \tag{3.11c}$$

where

$$\mathcal{F}_1 := -U_0^2 V_1/V_0^2. \tag{3.12}$$

Since V_1 is independent of U_1 and W_1, we solve Eq. (3.11b) for V_1 first to obtain

$$V_1 = c_{k,0}^2 g_1 + b_{k,1}y + c_{k,1}, \tag{3.13}$$

where $b_{k,1},\ c_{k,1}$ are constants left to be determined and g_1 is an even function defined as

$$g_1 := -\frac{1}{D}\int_0^y \int_0^z \rho^2 \,\mathrm{d}\hat{y}\mathrm{d}z. \tag{3.14}$$

The far field behavior of V_1 is

$$V_1 \to \left(c_{k,0}^2 g_1'(\pm\infty) + b_{k,1}\right) y + \left[c_{k,1} - \frac{c_{k,0}^2}{D}\int_0^{\pm\infty}\int_{\pm\infty}^{y} \rho^2 \,\mathrm{d}z\mathrm{d}y\right], \text{ as } y \to \pm\infty, \tag{3.15}$$

Since g_1' is odd, the constant $b_{k,1}$ can be determined by the far field behavior of V_1':

$$b_{k,1} = \frac{1}{2}\left(V_1'(+\infty) + V_1'(-\infty)\right). \tag{3.16}$$

Using Eq. (3.11c) to remove W_1 in Eq. (3.11a) yields

$$U_{1yy} - U_1 + 2\rho U_1 = -\mathcal{F}_1. \tag{3.17}$$

Since U_{0y} is the homogeneous solution of Eq. (3.17), the right-hand side of Eq. (3.17) must be orthogonal to U_{0y}. Taking the inner product between Eq. (3.17) and U_{0y} gives rise to the solvability condition of Eq. (3.17):

$$-\langle U_{0y}, \mathcal{F}_1\rangle = 0, \tag{3.18}$$

Using the fact that U_{0y} is odd and V_1 can be decomposed as the addition of odd and even functions, we obtain

$$b_{k,1}\int_{-\infty}^{\infty} \rho^2 \rho' y \mathrm{d}y = 0. \tag{3.19}$$

Thus, the solvability condition yields

$$b_{k,1} = 0. \tag{3.20}$$

Using Eq. (3.20), we solve Eq. (3.11a) for U_1 to obtain

$$U_1 = c_{k,1}\rho + c_{k,0}^2 f_1, \tag{3.21}$$

where f_1 is an even function satisfying

$$f_1'' - f_1 + 2\rho f_1 = \rho^2 g_1. \tag{3.22}$$

Taking the inner product between Eq. (3.11c) and U_{0y} and using the orthogonal condition Eq. (3.9) yield

$$\frac{\partial p_k}{\partial T_1} = \kappa\alpha_k. \tag{3.23}$$

Substituting Eq. (3.23) into Eq. (3.11c), we obtain

$$W_1 = U_1. \tag{3.24}$$

In the order of ε^2, we obtain

$$-U_{0y}\frac{\partial p_k}{\partial T_2} - U_{1y}\frac{\partial p_k}{\partial T_1} + \frac{\partial U_1}{\partial T_1} - \mathcal{F}_2 = U_{2yy} - (1-\kappa)U_2 + 2U_0U_2/V_0 - \kappa W_2, \tag{3.25a}$$

$$0 = DV_{2yy} - V_0 + 2U_0U_1, \tag{3.25b}$$

$$-W_{0y}\frac{\partial p_k}{\partial T_2} - (W_{1y} + \alpha_k U_{0yy})\frac{\partial p_k}{\partial T_1} + U_{0y}\frac{\partial \alpha_k}{\partial T_1} + \frac{\partial W_1}{\partial T_1} = \kappa(U_2 - W_2), \tag{3.25c}$$

where

$$\mathcal{F}_2 := U_1^2/V_0 - 2U_0U_1V_1/V_0^2 - U_0^2V_2/V_0^2 + U_0^2V_1^2/V_0^3. \tag{3.26}$$

Solving Eq. (3.25b) for V_2, we obtain

$$\begin{aligned} V_2 &= \frac{1}{D}\int_0^y\int_0^z (V_0 - 2U_0U_1)\,\mathrm{d}\hat{y}\mathrm{d}z + b_{k,2}y + c_{k,2} \\ &= \frac{1}{2D}c_{k,0}y^2 + b_{k,2}y + c_{k,2} + 2c_{k,0}c_{k,1}g_1 + 2c_{k,0}^3 g_2, \end{aligned} \tag{3.27}$$

where $b_{k,2},\ c_{k,2}$ are constants determined by matching with the outer region and g_2 is defined as

$$g_2 := -\frac{1}{D}\int_0^y\int_0^z \rho f_1\,\mathrm{d}\hat{y}\mathrm{d}z. \tag{3.28}$$

Note that $b_{k,2}$ can be determined by the far field behavior of V_2' as follows:

$$b_{k,2} = \frac{1}{2}\left(V_2'(+\infty) + V_2'(-\infty)\right). \tag{3.29}$$

Using Eqs. (3.25c) and (3.24) to remove W_2 in Eq. (3.25a) yields

$$U_{2yy} - U_2 + 2\rho U_2 = -\mathcal{F}_2 + U_{0yy}\frac{\partial p_k}{\partial T_1}\alpha_k - U_{0y}\frac{\partial \alpha_k}{\partial T_1}. \tag{3.30}$$

Taking the inner product between Eq. (3.30) and U_{0y} gives rise to

$$\frac{\partial \alpha_k}{\partial T_1} = -\frac{\langle \mathcal{F}_2, U_{0y}\rangle}{\langle U_{0y}, U_{0y}\rangle} + \frac{\langle U_{0yy}, U_{0y}\rangle}{\langle U_{0y}, U_{0y}\rangle}\frac{\partial p_k}{\partial T_1}\alpha_k. \tag{3.31}$$

Note that only the inner product between U_{0y} and the odd part of $\mathcal{F}_2$ is nonzero. We simplify Eq. (3.31) as

$$\frac{\partial \alpha_k}{\partial T_1} = \frac{b_{k,2}\int_{-\infty}^{\infty}\rho^2\rho' y\,\mathrm{d}y}{c_{k,0}\int_{-\infty}^{\infty}\rho'^2\,\mathrm{d}y}, \tag{3.32}$$

We rewrite U_2 as a summation of an even function and an odd function

$$U_2 = U_{2,e} + U_{2,o}, \tag{3.33}$$

where $U_{2,e}$ and $U_{2,o}$ satisfy:

$$\begin{aligned} U_{2,eyy} - U_{2,e} + 2\rho U_{2,e} &= -U_1^2/V_0 + 2U_0U_1V_1/V_0^2 + U_0^2 V_{2,e}/V_0^2 \\ &\quad -U_0^2V_1^2/V_0^3 + U_{0yy}\frac{\partial p_k}{\partial T_1}\alpha_k, \end{aligned} \tag{3.34}$$

$$U_{2,oyy} - U_{2,o} + 2\rho U_{2,o} = U_0^2 V_{2,o}/V_0^2 - U_{0y}\frac{\partial \alpha_k}{\partial T_1}. \tag{3.35}$$

For latter use, we express $U_{2,e}$ and $U_{2,o}$ as

$$\begin{aligned} U_{2,e} &= c_{k,1}c_{k,0}e_1 + c_{k,2}\rho + c_{k,0}e_2 + c_{k,0}^3 e_3 \\ &\quad + \frac{c_{k,0}\kappa\alpha_k^2}{2} y\rho', \end{aligned} \tag{3.36}$$

$$U_{2,o} = b_{k,2} f_2, \tag{3.37}$$

where $e_j,\ j = 1, \ldots, 3$, are even and f_2 is odd, satisfying

$$e_1'' - e_1 + 2\rho e_1 = 2\rho^2 g_1, \tag{3.38a}$$

$$e_2'' - e_2 + 2\rho e_2 = \frac{1}{2D}\rho^2 y^2, \tag{3.38b}$$

$$e_3'' - e_3 + 2\rho e_3 = -f_1^2 + 2\rho g_1 f_1 + 2\rho^2 g_2 - \rho^2 g_1^2, \tag{3.38c}$$

$$f_2'' - f_2 + 2\rho f_2 = \rho^2 y - \frac{\rho' \int_{-\infty}^{\infty} \rho^2 \rho' y \mathrm{d}y}{\int_{-\infty}^{\infty} \rho'^2 \,\mathrm{d}y}. \tag{3.38d}$$

Taking the inner product between Eq. (3.25c) and U_{0y} and using the orthogonal condition Eq. (3.9) yield

$$\frac{\partial p_k}{\partial T_2} = \frac{\partial \alpha_k}{\partial T_1} - \frac{\langle W_{1y} + \alpha_k U_{0yy}, U_{0y}\rangle}{\langle U_{0y}, U_{0y}\rangle}\frac{\partial p_k}{\partial T_1}. \tag{3.39}$$

Note that

$$\begin{aligned} \langle W_{1y} + \alpha_k U_{0yy}, U_{0y}\rangle &= \langle U_{1y} + \alpha_k U_{0yy}, U_{0y}\rangle = \langle U_{1y}, U_{0y}\rangle \\ &= c_{k,0}c_{k,1}\int_{-\infty}^{\infty} \rho'^2 \,\mathrm{d}y + c_{k,0}^3 \int_{-\infty}^{\infty} f_{1y}\rho' \,\mathrm{d}y. \end{aligned} \tag{3.40}$$

Thus,

$$\frac{\partial p_k}{\partial T_2} = \frac{b_{k,2}\int_{-\infty}^{\infty} \rho^2\rho' y \,\mathrm{d}y}{c_{k,0}\int_{-\infty}^{\infty} \rho'^2 \,\mathrm{d}y} - \frac{c_{k,1}\int_{-\infty}^{\infty} \rho'^2 \,\mathrm{d}y + c_{k,0}^2\int_{-\infty}^{\infty} f_{1y}\rho' \,\mathrm{d}y}{c_{k,0}\int_{-\infty}^{\infty} \rho'^2 \,\mathrm{d}y}\kappa\alpha_k. \tag{3.41}$$

Substituting Eq. (3.39) into Eq. (3.25c), we obtain

$$W_2 = U_2 + \frac{1}{\kappa}(W_{1y} + \alpha_k U_{0yy})\frac{\partial p_k}{\partial T_1} - \frac{1}{\kappa}\frac{\langle W_{1y}, U_{0y}\rangle}{\langle U_{0y}, U_{0y}\rangle}\frac{\partial p_k}{\partial T_1}U_{0y}. \tag{3.42}$$

In the order of ε^3, we obtain

$$-U_{0y}\frac{\partial p_k}{\partial T_3} - U_{1y}\frac{\partial p_k}{\partial T_2} + \frac{\partial U_1}{\partial T_2} + \frac{dU_2}{dT_1}$$
$$-\mathcal{F}_3 = U_{3yy} - (1-\kappa)U_3 + 2U_0U_3/V_0 - \kappa W_3, \tag{3.43a}$$
$$0 = DV_{3yy} - V_1 + 2U_0U_2 + U_1^2, \tag{3.43b}$$
$$-\hat{\tau}\kappa\frac{\partial p_k}{\partial T_1}U_{0y} - W_{0y}\frac{\partial p_k}{\partial T_3} - (W_{1y} + \alpha_k U_{0yy})\frac{\partial p_k}{\partial T_2} + U_{0y}\frac{\partial \alpha_k}{\partial T_2}$$
$$+\frac{\partial W_1}{\partial T_2} + \frac{dW_2}{dT_1} = \kappa(U_3 - W_3). \tag{3.43c}$$

where

$$\mathcal{F}_3 := \Big(2U_0^2V_1V_2 + 2U_1U_2V_0^2 + 2U_0U_1V_1^2 - 2U_0U_1V_0V_2$$
$$-(U_1^2 + 2U_0U_2)V_1V_0 - U_0^2V_3V_0 - U_0^2V_1^3/V_0\Big)/V_0^3. \tag{3.44}$$

Solving Eq. (3.43b), we obtain

$$V_3 = \frac{1}{D}\int_0^y\int_0^z (V_1 - 2U_0U_2 - U_1^2)\,\mathrm{d}\hat{y}\,\mathrm{d}z + b_{k,3}y + c_{k,3}, \tag{3.45}$$

where $b_{k,3},\ c_{k,3}$ are constants determined by matching with the outer region. We rewrite V_3 as the sum of an even function $V_{3,e}$ and an odd function $V_{3,o}$:

$$V_3 = V_{3,e} + V_{3,o}. \tag{3.46}$$

Then,

$$V_{3,o} = b_{k,3}y + 2b_{k,2}c_{k,0}g_3. \tag{3.47}$$

where g_3 is an odd function defined as

$$g_3 := -\frac{1}{D}\int_0^y\int_0^z \rho f_2\,\mathrm{d}\hat{y}\,\mathrm{d}z. \tag{3.48}$$

Note that $b_{k,3}$ can be determined by the far field behavior of V_3' as follows:

$$b_{k,3} = \frac{1}{2}\left(V_3'(+\infty) + V_3'(-\infty)\right) + \frac{2b_{k,2}c_{k,0}}{D}\int_0^\infty \rho f_2\,\mathrm{d}y. \tag{3.49}$$

Using Eq. (3.43c) to remove W_3 in Eq. (3.43a) yields

$$U_{3yy} - U_3 + 2\rho U_3 = \hat{\tau}\kappa \frac{\partial p_k}{\partial T_1} U_{0y} + \alpha_k U_{0yy} \frac{\partial p_k}{\partial T_2} - U_{0y} \frac{\partial \alpha_k}{\partial T_2} + \frac{d(U_2 - W_2)}{dT_1} - \mathcal{F}_3. \tag{3.50}$$

Taking the inner product between Eq. (3.50) and U_{0y} gives rise to

$$\frac{\partial \alpha_k}{\partial T_2} = \hat{\tau}\kappa \frac{\partial p_k}{\partial T_1} + \frac{\langle \frac{d(U_2 - W_2)}{dT_1}, U_{0y}\rangle}{\langle U_{0y}, U_{0y}\rangle} + \alpha_k \frac{\partial p_k}{\partial T_2} \frac{\langle U_{0y}, U_{0yy}\rangle}{\langle U_{0y}, U_{0y}\rangle} - \frac{\langle \mathcal{F}_3, U_{0y}\rangle}{\langle U_{0y}, U_{0y}\rangle}. \tag{3.51}$$

We now compute each of the terms on the right-hand side of Eq. (3.51). Integrating by parts and using Eqs. (3.9), (3.25c), (3.23), (3.24), we calculate

$$\begin{aligned} \langle \frac{d(U_2 - W_2)}{dT_1}, U_{0y}\rangle &= \frac{d}{dT_1}\langle U_2 - W_2, U_{0y}\rangle - \langle U_2 - W_2, -\frac{\partial p_k}{\partial T_1} U_{0yy}\rangle \\ &= 0 - \frac{1}{\kappa}\langle W_{1y} + \alpha_k U_{0yy}, U_{0yy}\rangle \left(\frac{\partial p_k}{\partial T_1}\right)^2 \\ &= -\kappa \alpha_k^3 \langle U_{0yy}, U_{0yy}\rangle. \end{aligned} \tag{3.52}$$

Using the fact that U_{0y} is odd and U_{0yy} is even, we obtain

$$\langle U_{0y}, U_{0yy}\rangle = 0. \tag{3.53}$$

Since the inner product between U_{0y} and the even part of $\mathcal{F}_3$ is 0, we calculate

$$\begin{aligned} \langle \mathcal{F}_3, U_{0y}\rangle &= \langle \frac{2V_{2,o}U_0^2 V_1 + 2U_{2,o}U_1 V_0^2 - 2V_{2,o}U_0 U_1 V_0 - 2U_{2,o}U_0 V_1 V_0 - U_0^2 V_{3,o} V_0}{V_0^3}, U_{0y}\rangle \\ &= c_{k,0}^2 b_{k,2} I_1 - c_{k,0} b_{k,3} I_2, \end{aligned} \tag{3.54}$$

where

$$I_1 = \int_{-\infty}^{\infty} 2\left[(y\rho - f_2)(\rho g_1 - f_1) - g_3\rho^2\right]\rho' \mathrm{d}y, \quad I_2 = \int_{-\infty}^{\infty} y\rho^2\rho' \mathrm{d}y. \tag{3.55}$$

Thus,

$$\frac{\partial \alpha_k}{\partial T_2} = \hat{\tau}\kappa^2 \alpha_k - \frac{\kappa \int_{-\infty}^{\infty} (\rho'')^2 \,\mathrm{d}y}{\int_{-\infty}^{\infty} \rho'^2 \,\mathrm{d}y} \alpha_k^3 - \frac{c_{k,0} b_{k,2} I_1 - b_{k,3} I_2}{c_{k,0} \int_{-\infty}^{\infty} \rho'^2 \,\mathrm{d}y}. \tag{3.56}$$

We summarize the equations for p_k and α_k at the first two time scales as follows:

$$\frac{\partial p_k}{\partial T_1} = \kappa\alpha_k, \tag{3.57a}$$

$$\frac{\partial \alpha_k}{\partial T_1} = \frac{b_{k,2}\int_{-\infty}^{\infty}\rho^2\rho' y\,\mathrm{d}y}{c_{k,0}\int_{-\infty}^{\infty}\rho'^2\,\mathrm{d}y}, \tag{3.57b}$$

$$\frac{\partial p_k}{\partial T_2} = \frac{b_{k,2}\int_{-\infty}^{\infty}\rho^2\rho' y\,\mathrm{d}y}{c_{k,0}\int_{-\infty}^{\infty}\rho'^2\,\mathrm{d}y} - \frac{c_{k,1}\int_{-\infty}^{\infty}\rho'^2\,\mathrm{d}y + c_{k,0}^2\int_{-\infty}^{\infty} f_{1y}\rho'\,\mathrm{d}y.}{c_{k,0}\int_{-\infty}^{\infty}\rho'^2\,\mathrm{d}y}\kappa\alpha_k, \tag{3.57c}$$

$$\frac{\partial \alpha_k}{\partial T_2} = \hat{\tau}\kappa^2\alpha_k - \frac{\kappa\int_{-\infty}^{\infty}(\rho'')^2\,\mathrm{d}y}{\int_{-\infty}^{\infty}\rho'^2\,\mathrm{d}y}\alpha_k^3 - \frac{c_{k,0}b_{k,2}I_1 - b_{k,3}I_2}{c_{k,0}\int_{-\infty}^{\infty}\rho'^2\,\mathrm{d}y}. \tag{3.57d}$$

Thus, Eq. (3.4) becomes

$$\dot{p}_k = \kappa\alpha_k\varepsilon + \left(\frac{b_{k,2}\int_{-\infty}^{\infty}\rho^2\rho' y\,\mathrm{d}y}{c_{k,0}\int_{-\infty}^{\infty}\rho'^2\,\mathrm{d}y} - \frac{c_{k,1}\int_{-\infty}^{\infty}\rho'^2\,\mathrm{d}y + c_{k,0}^2\int_{-\infty}^{\infty} f_{1y}\rho'\,\mathrm{d}y}{c_{k,0}\int_{-\infty}^{\infty}\rho'^2\,\mathrm{d}y}\kappa\alpha_k\right)\varepsilon^2 + \mathcal{O}(\varepsilon^3), \tag{3.58a}$$

$$\dot{\alpha}_k = \frac{b_{k,2}\int_{-\infty}^{\infty}\rho^2\rho' y\,\mathrm{d}y}{c_{k,0}\int_{-\infty}^{\infty}\rho'^2\,\mathrm{d}y}\varepsilon + \left(\hat{\tau}\kappa^2\alpha_k - \frac{\kappa\int_{-\infty}^{\infty}(\rho'')^2\,\mathrm{d}y}{\int_{-\infty}^{\infty}\rho'^2\,\mathrm{d}y}\alpha_k^3 - \frac{c_{k,0}b_{k,2}I_1 - b_{k,3}I_2}{c_{k,0}\int_{-\infty}^{\infty}\rho'^2\,\mathrm{d}y}\right)\varepsilon^2 + \mathcal{O}(\varepsilon^3). \tag{3.58b}$$

Remark 1 The system (3.58) describes the dynamics of centers of N spikes when our initial condition is close to the quasi-equilibrium solution, in which $b_{k,2}$, $b_{k,3}$, $c_{k,0}$ and $c_{k,1}$ encode the information from other spikes and need to be determined from the outer solution.

Outer region: Away from the spike centers where x satisfies $|x - \hat{x}_k| \sim \mathcal{O}(1)$, u is exponentially small and v satisfies $Dv_{xx} - v \sim 0$ on the interval $x \in [-1, 1]$ with suitable discontinuity conditions imposed across $\hat{x}_k$. In the limit $\varepsilon \to 0$, the even part of $\frac{u^2}{\varepsilon}$ behaves in the distributional sense as a linear combination of $\delta(x - \hat{x}_k)$ for $k = 1, \ldots, N$, where $\delta(x)$ is the Dirac delta function. Whereas the odd part of $\frac{u^2}{\varepsilon}$ behaves like a linear combination of $\delta'(x - \hat{x}_k)$ for $k = 1, \ldots, N$. Therefore, v satisfies

$$Dv_{xx} - v + \sum_{k=1}^{N}\left(s_k\delta(x - x_k - \varepsilon p_k) + \varepsilon^2 h_k\delta'(x - x_k - \varepsilon p_k)\right) = 0, \quad v'(\pm 1) = 0, \tag{3.59}$$

where

$$
\begin{aligned}
s_k &= s_{k,0} + s_{k,1}\varepsilon + \cdots \\
&= \int_{-\infty}^{\infty} U_0^2 \mathrm{d}y + \varepsilon \int_{-\infty}^{\infty} 2U_0U_1 \,\mathrm{d}y + \varepsilon^2 \int_{-\infty}^{\infty} (U_1^2 + 2U_0U_{2,e}) \,\mathrm{d}y + \mathcal{O}(\varepsilon^3) \\
&= c_{k,0}^2 \int_{-\infty}^{\infty} \rho^2 \,\mathrm{d}y + \varepsilon \left(2c_{k,0}c_{k,1} \int_{-\infty}^{\infty} \rho^2 \,\mathrm{d}y + 2c_{k,0}^3 \int_{-\infty}^{\infty} \rho f_1 \,\mathrm{d}y \right) \\
&\quad + \varepsilon^2 \left(c_{k,1}^2 \int_{-\infty}^{\infty} \rho^2 \,\mathrm{d}y + 2c_{k,1}c_{k,0}^2 \int_{-\infty}^{\infty} \rho f_1 \,\mathrm{d}y \right. \\
&\quad + c_{k,0}^4 \int_{-\infty}^{\infty} f_1^2 \,\mathrm{d}y + 2c_{k,1}c_{k,0}^2 \int_{-\infty}^{\infty} \rho e_1 \,\mathrm{d}y + 2c_{k,2}c_{k,0} \int_{-\infty}^{\infty} \rho^2 \,\mathrm{d}y \\
&\quad + 2c_{k,0}^2 \int_{-\infty}^{\infty} (\rho e_2 + \frac{\kappa\alpha_k^2}{2} y\rho\rho') \,\mathrm{d}y \\
&\quad \left. + 2c_{k,0}^4 \int_{-\infty}^{\infty} \rho e_3 \,\mathrm{d}y \right) + \mathcal{O}(\varepsilon^3),
\end{aligned}
\tag{3.60}
$$

$$
\begin{aligned}
h_k &= h_{k,0} + \varepsilon h_{k,1} + \cdots \\
&= \int_{-\infty}^{\infty} \int_{\infty}^{z} 2U_0U_{2,o} \,\mathrm{d}\hat{y}\mathrm{d}z + \mathcal{O}(\varepsilon) \\
&= 2c_{k,0}b_{k,2} \int_{-\infty}^{+\infty} \int_{+\infty}^{z} \rho f_2 \,\mathrm{d}\hat{y}\mathrm{d}z + \mathcal{O}(\varepsilon).
\end{aligned}
\tag{3.61}
$$

Solving Eq. (3.59) yields

$$
v = \sum_{k=1}^{N} s_k G(x; x_k + \varepsilon p_k) - \varepsilon^2 \sum_{k=1}^{N} h_k G_z(x; x_k + \varepsilon p_k), \tag{3.62}
$$

where $G(x; z)$ is the Green's function satisfying

$$
DG_{xx} - G = -\delta(x - z), \quad G_x(\pm 1) = 0, \tag{3.63}
$$

and $G_z(x; z)$ is the derivative of Green's function with respect to the second variable, which satisfies

$$
DG_{zxx} - G_z = \delta'(x - z), \quad G_{zx}(\pm 1) = 0. \tag{3.64}
$$

A simple calculation gives:

$$
G(x; z) = \frac{1}{\sqrt{D}\sinh(2/\sqrt{D})} \begin{cases} \cosh\left(\frac{1-z}{\sqrt{D}}\right)\cosh\left(\frac{1+x}{\sqrt{D}}\right), & -1 < x < z, \\ \cosh\left(\frac{1+z}{\sqrt{D}}\right)\cosh\left(\frac{1-x}{\sqrt{D}}\right), & z < x < 1. \end{cases} \tag{3.65}
$$

For convenience, we rewrite G as

$$
G = \frac{1}{2\sqrt{D}} e^{-|x-z|/\sqrt{D}} + R(x; z), \tag{3.66}
$$

where R is the regular part of Green's function. Then, near the k-th spike $x = x_k + \varepsilon(p_k + y)$, we have

$$
\begin{aligned}
v(x) =& \sum_{j=1}^{N} s_j G(x_k + \varepsilon y + \varepsilon p_k; x_j + \varepsilon p_j) - \varepsilon^2 \sum_{j=1}^{N} h_j G_z(x_k + \varepsilon y + \varepsilon p_k; x_j + \varepsilon p_j) \\
=& v_{k,0}(y) + \varepsilon v_{k,1}(y) + \varepsilon^2 v_{k,2}(y) + \varepsilon^3 v_{k,3}(y) + \cdots
\end{aligned} \tag{3.67}
$$

where

$$
v_{k,0} = \sum_{j=1}^{N} s_{j,0} G(x_k; x_j), \tag{3.68}
$$

$$
\begin{aligned}
v_{k,1} =& \sum_{j=1}^{N} s_{j,1} G(x_k; x_j) + \sum_{j=1}^{N} s_{j,0} \\
& \left[G_x(x_k; x_j) p_k + G_z(x_k; x_j) p_j\right] + y \sum_{j=1}^{N} s_{j,0} G_x(x_k^{\pm}; x_j).
\end{aligned} \tag{3.69}
$$

Since only the derivatives of $v_{k,2}$ and $v_{k,3}$ at $y = 0$ are needed in the later matching procedure, we compute $\frac{\partial v_{k,2}(0^{\pm})}{\partial y}$ and $\frac{\partial v_{k,3}(0^{\pm})}{\partial y}$ as follows,

$$
\frac{\partial v_{k,2}(0^{\pm})}{\partial y} = \sum_{j=1}^{N} \left(s_{j,0} \left[G_{xx}(x_k^{\pm}; x_j) p_k + G_{zx}(x_k^{\pm}; x_j) p_j\right] + s_{j,1} G_x(x_k^{\pm}; x_j) \right), \tag{3.70}
$$

$$
\begin{aligned}
\frac{\partial v_{k,3}(0^{\pm})}{\partial y} =& \sum_{j=1}^{N} \Big(\frac{1}{6} s_{j,0} \left[3G_{xxx}(x_k^{\pm}; x_j) p_k^2 + 6G_{zxx}(x_k^{\pm}; x_j) p_k p_j + 3G_{zzx}(x_k^{\pm}; x_j) p_j^2\right] \\
& + s_{j,1} \left[G_{xx}(x_k^{\pm}; x_j) p_k + G_{zx}(x_k^{\pm}; x_j) p_j\right] + s_{j,2} G_x(x_k^{\pm}; x_j) - h_{j,0} G_{zx}(x_k^{\pm}; x_j) \Big).
\end{aligned} \tag{3.71}
$$

Matching: To determine the constants in the inner region, we match the local behavior of the solution v with the far field behavior of V in each order of ε. For convenience, we define the matrix $\mathcal{G}$ as

$$
\mathcal{G} = (G(x_k; x_j)). \tag{3.72}
$$

Let us denote $\frac{\partial}{\partial x_k}$ as ∇_{x_k}. When $k \neq j$, we can define $\nabla_{x_k} G(x_k; x_j)$ and $\nabla_{x_j} G(x_k; x_j)$ in the classical way. When $k = j$, we define

$$
\nabla_{x_k} G(x_k; x_k) := \frac{\partial}{\partial x}\Big|_{x=x_k} R(x; x_k). \tag{3.73}
$$

We also define the matrix $\mathcal{P}$ and $\mathcal{G}_g$ as follows,

$$\mathcal{P} := \left(\nabla_{x_k} G(x_k; x_j)\right), \tag{3.74}$$

$$\mathcal{G}_g := \left(\nabla_{x_j} \nabla_{x_k} G(x_k; x_j)\right). \tag{3.75}$$

As we have chosen x_k as the equilibrium position of the k-th spike, we have the following identities related to G from Iron et al. (2001):

$$\sum_{j=1}^{N} G(x_k; x_j) = c_g, \tag{3.76a}$$

$$\sum_{j=1}^{N} \nabla_{x_k} G(x_k; x_j) = 0, \qquad \sum_{k=1}^{N} \nabla_{x_j} G(x_k; x_j) = 0,$$

$$\nabla_{x_k} G(x_k; x_j) = \nabla_{x_k} G(x_j; x_k). \tag{3.76b}$$

where $c_g := \left[2\sqrt{D}\tanh\left(\frac{1}{\sqrt{D}N}\right)\right]^{-1}$ is a constant independent of k.

Matching the term in the leading order, we obtain

$$c_{k,0} = \sum_{j=1}^{N} s_{j,0} G(x_k; x_j). \tag{3.77}$$

We assume N spikes have the same height in the leading order, then $c_{k,0}$ has the same value for $k = 1, \ldots, N$. Using Eq. (3.76a), we solve Eq. (3.77) to obtain

$$c_{k,0} = \frac{1}{c_g \int_{-\infty}^{\infty} \rho^2 \, \mathrm{d}y}. \tag{3.78}$$

Matching the terms in the order ε, we obtain

$$b_{k,1} = \frac{1}{2}\left(V_1'(+\infty) + V_1'(-\infty)\right) = \frac{1}{2}\left(\frac{\partial v_{k,1}(0^+)}{\partial y} + \frac{\partial v_{k,1}(0^-)}{\partial y}\right)$$

$$= \sum_{j=1}^{N} s_{j,0} \nabla_{x_k} G(x_k; x_j), \tag{3.79}$$

and

$$
\begin{aligned}
c_{k,1} &= v_{k,1}(0) + \frac{c_{k,0}^2}{D}\int_0^{+\infty}\int_{+\infty}^{y}\rho^2\,\mathrm{d}z\mathrm{d}y \\
&= \sum_{j=1}^{N} s_{j,1}G(x_k;x_j) + \sum_{j=1}^{N} s_{j,0}\left[\nabla_{x_k}G(x_k;x_j)p_k + \nabla_{x_j}G(x_k;x_j)p_j\right] \\
&\quad + \frac{c_{k,0}^2}{D}\int_0^{+\infty}\int_{+\infty}^{y}\rho^2\,\mathrm{d}z\mathrm{d}y.
\end{aligned}
\tag{3.80}
$$

Substituting Eq. (3.76b) into Eq. (3.79), we obtain

$$
b_{k,1} = 0, \tag{3.81}
$$

which is consistent with the solvability condition Eq. (3.20) in the inner region. Using Eqs. (3.76a) and (3.76b), we can rewrite Eq. (3.80) in the form

$$
\left(-\frac{2}{c_g}\mathcal{G}+\mathcal{I}\right)\mathbf{c}_1 = \frac{1}{c_g^2\int_{-\infty}^{\infty}\rho^2\,\mathrm{d}y}\left(\mathcal{P}^{\mathsf{T}}\mathbf{p} + \tilde{c}\mathbf{1}_N\right), \tag{3.82}
$$

where $\mathcal{I}$ is the identity matrix, $\mathbf{p} := [p_1, p_2, \cdots, p_N]^{\mathsf{T}}$, $\mathbf{c_1} := [c_{1,1}, c_{2,1}, \cdots, c_{N,1}]^{\mathsf{T}}$, $\mathbf{1}_N = [1, 1, \cdots, 1]^{\mathsf{T}}$ and

$$
\tilde{c} = \left(\int_{-\infty}^{+\infty}\rho^2\mathrm{d}y\right)^{-1}\left(\frac{1}{D}\int_0^{+\infty}\int_{+\infty}^{y}\rho^2\,\mathrm{d}z\mathrm{d}y + 2\left(\int_{-\infty}^{+\infty}\rho^2\mathrm{d}y\right)^{-1}\int_{-\infty}^{+\infty}\rho f_1\mathrm{d}y\right). \tag{3.83}
$$

Using $\left(-\frac{2}{c_g}\mathcal{G}+\mathcal{I}\right)^{-1}\mathbf{1}_N = -\mathbf{1}_N$, we can express $\mathbf{c}_1$ as

$$
\mathbf{c}_1 = \frac{1}{c_g^2\int_{-\infty}^{\infty}\rho^2\,\mathrm{d}y}\left(\left(-\frac{2}{c_g}\mathcal{G}+\mathcal{I}\right)^{-1}\mathcal{P}^{\mathsf{T}}\mathbf{p} - \tilde{c}\mathbf{1}_N\right). \tag{3.84}
$$

Matching the terms in the order of ε^2, we obtain

$$
\begin{aligned}
b_{k,2} &= \frac{1}{2}\left(V_2'(+\infty) + V_2'(-\infty)\right) \\
&= \frac{1}{2}\left(\frac{\partial v_{k,2}(0^+)}{\partial y} + \frac{\partial v_{k,2}(0^-)}{\partial y}\right) \\
&= \sum_{j=1}^{N}\left(s_{j,0}\left[\nabla_{x_k}\nabla_{x_k}G(x_k;x_j)p_k + \nabla_{x_j}\nabla_{x_k}G(x_k;x_j)p_j\right] + s_{j,1}\nabla_{x_k}G(x_k;x_j)\right).
\end{aligned}
\tag{3.85}
$$

Using the fact that $\sum_{j=1}^{N}\nabla_{x_k}\nabla_{x_k}G(x_k;x_j)=\frac{1}{D}\sum_{j=1}^{N}G(x_k;x_j)=\frac{c_g}{D}$ and $\mathcal{P}\mathbf{1}_N=0$, Eq. (3.85) becomes

$$
\begin{aligned}
\mathbf{b}_2 &= \frac{1}{c_g^2\int_{-\infty}^{\infty}\rho^2\,\mathrm{d}y}\left(\frac{c_g}{D}I+\mathcal{G}_g\right)\mathbf{p}+\frac{2}{c_g}\mathcal{P}\mathbf{c}_1 \\
&= \frac{1}{c_g^2\int_{-\infty}^{\infty}\rho^2\,\mathrm{d}y}\left(\frac{c_g}{D}\mathcal{I}+\mathcal{G}_g+\frac{2}{c_g}\mathcal{P}\left(-\frac{2}{c_g}\mathcal{G}+\mathcal{I}\right)^{-1}\mathcal{P}^{\mathsf{T}}\right)\mathbf{p}.
\end{aligned}
\tag{3.86}
$$

Matching the constant terms in the order of ε^2, we obtain

$$
\begin{aligned}
c_{k,2} =& \frac{1}{2}\sum_{j=1}^{N}s_{j,0}\left[\nabla_{x_k}\nabla_{x_k}G(x_k;x_j)p_k^2+2\nabla_{x_k}\nabla_{x_j}G(x_k;x_j)p_kp_j+\nabla_{x_j}\nabla_{x_j}G(x_k;x_j)p_j^2\right] \\
&+\sum_{j=1}^{N}s_{j,1}\left[\nabla_{x_k}G(x_k;x_j)p_k+\nabla_{x_j}G(x_k;x_j)p_j\right]+\sum_{j=1}^{N}s_{j,2}G(x_k;x_j) \\
&+\frac{2c_{k,0}c_{k,1}}{D}\int_0^{+\infty}\int_{+\infty}^{y}\rho^2\,\mathrm{d}z\mathrm{d}y \\
&+\frac{2c_{k,0}^3}{D}\int_0^{+\infty}\int_{+\infty}^{y}\rho f_1\,\mathrm{d}z\mathrm{d}y.
\end{aligned}
\tag{3.87}
$$

Matching the terms in the order of ε^3, we obtain

$$
\begin{aligned}
b_{k,3} &= \frac{1}{2}\left(V_3'(+\infty)+V_3'(-\infty)\right)+\frac{2c_{k,0}b_{k,2}}{D}\int_0^{\infty}\rho f_2\,\mathrm{d}y \\
&= \frac{1}{2}\left(\frac{\partial v_{k,3}(0^+)}{\partial y}+\frac{\partial v_{k,3}(0^-)}{\partial y}\right)+\frac{2c_{k,0}b_{k,2}}{D}\int_0^{\infty}\rho f_2\,\mathrm{d}y \\
&= \sum_{j=1}^{N}\Big(\frac{1}{2}s_{j,0}\Big[\nabla_{x_k}\nabla_{x_k}\nabla_{x_k}G(x_k;x_j)p_k^2+2\nabla_{x_j}\nabla_{x_k}\nabla_{x_k}G(x_k;x_j)p_kp_j \\
&\quad +\nabla_{x_j}\nabla_{x_j}\nabla_{x_k}G(x_k;x_j)p_j^2\Big] \\
&\quad +s_{j,1}\left[\nabla_{x_k}\nabla_{x_k}G(x_k;x_j)p_k+\nabla_{x_j}\nabla_{x_k}G(x_k;x_j)p_j\right] \\
&\quad +s_{j,2}\nabla_{x_k}G(x_k;x_j)-h_{j,0}\nabla_{x_j}\nabla_{x_k}G(x_k^{\pm};x_j)\Big) \\
&\quad +\frac{2c_{k,0}b_{k,2}}{D}\int_0^{\infty}\rho f_2\,\mathrm{d}y.
\end{aligned}
\tag{3.88}
$$

Observe that $c_{k,2}$ and $b_{k,3}$ consist of quadratic terms and linear terms involving p_j, $j=1,\cdots,N$, which will be eliminated in determining the ODE for the slow evolution of the amplitude in the later subsection. Hence, we omit the exact evaluations of them.

The constants in Eq. (3.58) have been determined explicitly. Thus, the dynamics of spikes' centers in the vicinity of Hopf bifurcations is governed by the system

(3.58), where the constants $c_{k,0}$, $c_{k,1}$, $c_{k,2}$, $b_{k,1}$, $b_{k,2}$, $b_{k,3}$ are determined by Eqs. (3.78) (3.84) (3.87) (3.81) (3.86) and (3.88). We do not intend to solve the full system but seek a leading order approximation in the order of ε.

3.2 Leading Order Periodic Solution

Equation (3.58) can be seen as a linear system with weakly nonlinear parts. We proceed to determine the leading order dynamics of Eq. (3.58). We denote

$$\mathcal{M} = \frac{c_g}{D}\mathcal{I} + \mathcal{G}_g + \frac{2}{c_g}\mathcal{P}\left(-\frac{2}{c_g}\mathcal{G} + \mathcal{I}\right)^{-1}\mathcal{P}^{\mathsf{T}}. \tag{3.89}$$

Substituting Eq. (3.58a) into Eq. (3.58b) and using the slow time $t_1 = \varepsilon t$, we can obtain a second- order nonlinear ODE system:

$$\frac{\mathrm{d}^2\mathbf{p}}{\mathrm{d}t_1^2} - \kappa\beta_1\mathcal{M}\mathbf{p} = \varepsilon\left((\hat{\tau}\kappa^2\mathcal{I} + \beta_1\mathcal{M})\frac{\mathrm{d}\mathbf{p}}{\mathrm{d}t_1} - \frac{\beta_2}{\kappa}\left(\frac{\mathrm{d}\mathbf{p}}{\mathrm{d}t_1}\right)^{\circ 3} + \frac{\mathrm{d}\mathbf{F}}{\mathrm{d}t_1} + \mathbf{H}\right), \tag{3.90}$$

where $[\ \sim\ ]^{\circ 3}$ is the Hadamard power, β_1 and β_2 are constants

$$\beta_1 := \frac{\int_{-\infty}^{\infty}\rho^2\rho' y\,\mathrm{d}y}{c_g\int_{-\infty}^{\infty}\rho'^2\,\mathrm{d}y} = -\frac{2}{c_g},\quad \beta_2 := \frac{\int_{-\infty}^{\infty}(\rho'')^2\,\mathrm{d}y}{\int_{-\infty}^{\infty}\rho'^2\,\mathrm{d}y} = \frac{5}{7}, \tag{3.91}$$

$\mathbf{F}\left(\mathbf{p}, \frac{\mathrm{d}\mathbf{p}}{\mathrm{d}t_1}\right)$ and $\mathbf{H}\left(\mathbf{p}, \frac{\mathrm{d}\mathbf{p}}{\mathrm{d}t_1}\right)$ are vectors defined as

$$\mathbf{F} = \begin{bmatrix} F_1 \\ F_2 \\ \vdots \\ F_N \end{bmatrix},\quad \mathbf{H} = \begin{bmatrix} H_1 \\ H_2 \\ \vdots \\ H_N \end{bmatrix}, \tag{3.92}$$

with

$$F_k = -\frac{c_{k,1}\int_{-\infty}^{\infty}\rho'^2\,\mathrm{d}y + c_{k,0}^2\int_{-\infty}^{\infty} f_{1y}\rho'\,\mathrm{d}y.}{c_{k,0}\int_{-\infty}^{\infty}\rho'^2\,\mathrm{d}y}\kappa\alpha_k,\quad H_k = -\kappa\frac{c_{k,0}b_{k,2}I_1 - b_{k,3}I_2}{c_{k,0}\int_{-\infty}^{\infty}\rho'^2\,\mathrm{d}y}. \tag{3.93}$$

The eigenvalues of the matrix $\mathcal{M}$ are crucial to determine the dynamics. In Iron et al. (2001) (see Eq. (4.58)), the eigenvalues and eigenvectors of $\mathcal{M}$ are computed analytically. We summarize the result as follows:

Lemma 1 *The eigenvalue ζ_k of $\mathcal{M}$ are*

$$\zeta_k = \frac{c_g}{D} - \frac{1}{D^{\frac{3}{2}}\nu_k} + \frac{2}{D^{\frac{3}{2}}\nu_k\left(c_g\sqrt{D}\nu_k - 2\right)}\operatorname{csch}^2\left(\frac{2}{\sqrt{D}N}\right)\sin^2\left(\frac{\pi k}{N}\right), \tag{3.94}$$

with $\nu_k = 2\coth\left(\frac{2}{\sqrt{DN}}\right) - 2\mathrm{csch}\left(\frac{2}{\sqrt{DN}}\right)\cos\left(\frac{\pi k}{N}\right)$ *and the associated normalized eigenvectors* $\mathbf{q}_k$ *of* $\mathcal{M}$ *are defined in Eq. (2.11). These eigenvalues are positive and ordered as* $\zeta_N > \cdots > \zeta_2 > \zeta_1 > 0$ *only when* $D < D_N^*$*, where*

$$D_N^* := \frac{1}{N^2 \ln^2(1+\sqrt{2})}. \tag{3.95}$$

Remark 2 The terms $\frac{c_g}{D}$, $-\frac{1}{D^{\frac{3}{2}}\nu_k}$, and $\frac{2}{D^{\frac{3}{2}}\nu_k\left(c_g\sqrt{D}\nu_k-2\right)}\mathrm{csch}^2\left(\frac{2}{\sqrt{DN}}\right)\sin^2\left(\frac{\pi k}{N}\right)$ are eigenvalues of the matrices $\frac{c_g}{D}\mathcal{I}$, $\mathcal{G}_g$, and $\frac{2}{c_g}\mathcal{P}\left(-\frac{2}{c_g}\mathcal{G}+\mathcal{I}\right)^{-1}\mathcal{P}^\mathsf{T}$, respectively. The order of ζ_k when $D < D_N^*$ is not mentioned in the reference (Iron et al. 2001), but we can see it by further simplifying ζ_k as

$$\zeta_k = \frac{c_g}{D}\frac{\left(1-\cos\left(\frac{k\pi}{N}\right)\right)\left(1-2\tanh^2\left(\frac{1}{\sqrt{DN}}\right)\right)}{2-\cosh\left(\frac{2}{\sqrt{DN}}\right)-\cos\left(\frac{k\pi}{N}\right)}. \tag{3.96}$$

Note that D_N^* corresponds to the zero of the term $\left(1-2\tanh^2\left(\frac{1}{\sqrt{DN}}\right)\right)$.

Remark 3 An N-spike equilibrium solution will be stable only when $D < D_N^*$. As we assume N-spike equilibria are stable at $\tau = 0$, the condition $D < D_N^*$ is implicitly required.

Let $\boldsymbol{\xi} = Q^\mathsf{T}\mathbf{p}$, then Eq. (3.90) becomes

$$\frac{\mathrm{d}^2\boldsymbol{\xi}}{\mathrm{d}t_1^2} - \kappa\beta_1\Lambda\boldsymbol{\xi} = \varepsilon\left((\hat{\tau}\kappa^2\mathcal{I}+\beta_1\Lambda)\frac{\mathrm{d}\boldsymbol{\xi}}{\mathrm{d}t_1} - \frac{\beta_2}{\kappa}Q^\mathsf{T}\left(Q\frac{\mathrm{d}\boldsymbol{\xi}}{\mathrm{d}t_1}\right)^{\circ 3} + Q^\mathsf{T}\frac{\mathrm{d}\mathbf{F}\left(Q\boldsymbol{\xi}, Q\frac{\mathrm{d}\boldsymbol{\xi}}{\mathrm{d}t_1}\right)}{\mathrm{d}t_1}\right.$$
$$\left. + Q^\mathsf{T}\mathbf{H}\left(Q\boldsymbol{\xi}, Q\frac{\mathrm{d}\boldsymbol{\xi}}{\mathrm{d}t_1}\right)\right), \tag{3.97}$$

where Λ is the diagonal matrix with ζ_k on its diagonal. Next, we derive a multiple-scale approximation of the solution to Eq. (3.97). We introduce slow time scales $t_2 = \varepsilon t_1$ and assume

$$\boldsymbol{\xi} = \boldsymbol{\xi}_0(t_1, t_2) + \varepsilon\boldsymbol{\xi}_1(t_1, t_2) + \cdots. \tag{3.98}$$

Then,

$$\frac{\mathrm{d}\boldsymbol{\xi}}{\mathrm{d}t_1} = \frac{\partial\boldsymbol{\xi}_0}{\partial t_1} + \varepsilon\left(\frac{\partial\boldsymbol{\xi}_1}{\partial t_1} + \frac{\partial\boldsymbol{\xi}_0}{\partial t_2}\right) + \mathcal{O}(\varepsilon^2). \tag{3.99}$$

Substituting Eq. (3.98) into Eq. (3.97) and collecting terms in the leading order yield

$$\frac{\partial^2\boldsymbol{\xi}_0}{\partial t_1^2} - \kappa\beta_1\Lambda\boldsymbol{\xi}_0 = 0. \tag{3.100}$$

The general solution of this problem is

$$\boldsymbol{\xi}_0 = \begin{bmatrix} B_1(t_2)\cos(\omega_1 t_1 + \theta_1(t_2)) \\ B_2(t_2)\cos(\omega_2 t_1 + \theta_2(t_2)) \\ \vdots \\ B_N(t_2)\cos(\omega_N t_1 + \theta_N(t_2)) \end{bmatrix}, \tag{3.101}$$

where

$$\omega_k = \sqrt{-\kappa\beta_1\zeta_k}\ , \tag{3.102}$$

$B_k(t_2)$ and $\theta_k(t_2)$ are functions of slow time scale t_2 that need to be determined in the $\mathcal{O}(\varepsilon)$ equation. In the order of ε, we have

$$\begin{aligned} \frac{\partial^2 \boldsymbol{\xi}_1}{\partial t_1^2} - \kappa\beta_1\Lambda\boldsymbol{\xi}_1 &= -2\frac{\partial^2\boldsymbol{\xi}_0}{\partial t_1 \partial t_2} \\ &+ \left((\hat{\tau}\kappa^2\mathcal{I} + \beta_1\Lambda)\frac{\partial \boldsymbol{\xi}_0}{\partial t_1} - \frac{\beta_2}{\kappa} Q^{\mathsf{T}} \left(Q\frac{\partial\boldsymbol{\xi}_0}{\partial t_1}\right)^{\circ 3} + Q^{\mathsf{T}} \frac{\partial \mathbf{F}\left(Q\boldsymbol{\xi}_0, Q\frac{\partial\boldsymbol{\xi}_0}{\partial t_1}\right)}{\partial t_1} \right. \\ &\left. + Q^{\mathsf{T}}\mathbf{H}\left(Q\boldsymbol{\xi}_0, Q\frac{\partial\boldsymbol{\xi}_0}{\partial t_1}\right)\right). \end{aligned} \tag{3.103}$$

Note that Eq. (3.103) can be decoupled into N independent second-order inhomogeneous ODEs. To obtain a bounded solution for each element of $\boldsymbol{\xi}_1$, we need to remove the secular terms (the solutions of the associated homogeneous equation) in the inhomogeneous part. A careful examination shows that $Q^{\mathsf{T}}\frac{\partial \mathbf{F}\left(Q\boldsymbol{\xi}_0, Q\frac{\partial\boldsymbol{\xi}_0}{\partial t_1}\right)}{\partial t_1}$ and $Q^{\mathsf{T}}\mathbf{H}\left(Q\boldsymbol{\xi}_0, Q\frac{\partial\boldsymbol{\xi}_0}{\partial t_1}\right)$ contain no secular terms involving $\sin(\omega_k t_1 + \theta_k(t_2))$ in the k-th component of Eq. (3.103). Then, by removing the secular term involving $\sin(\omega_k t_1 + \theta_k(t_2))$ in the k-th component, we obtain the equations for the amplitude of $\xi_{0,k}$

$$\frac{\mathrm{d}B_k}{\mathrm{d}t_2} = B_k\left[\frac{1}{2}(\hat{\tau}\kappa^2 + \beta_1\zeta_k) - \frac{3\beta_2}{8\kappa N}\sum_{j=1}^{N} a_{k,j}\omega_j^2 B_j^2\right], \tag{3.104}$$

where

$$a_{k,j} = \begin{cases} N\sum_{l=1}^{N} Q_{lj}^4 & j = k \\ 2N\sum_{l=1}^{N} Q_{lj}^2 Q_{lk}^2 & j \neq k \end{cases}. \tag{3.105}$$

Remark 4 We can obtain the equation of $\theta_k(t_2)$ by removing the secular terms involving $\cos(\omega_k t_1 + \theta_k(t_2))$ in the k-th component of Eq. (3.103). In this situation, $\mathbf{F}$ and $\mathbf{H}$ will contribute to the secular term. As we are interested in the amplitude system that is critical to the manifestation of the periodic orbit, we will not go into details here.

Remark 5 Note that $\beta_1\zeta_k$ are the eigenvalues of the system at $\tau = 0$. Hence, the system (3.104) is the same as the corresponding amplitude equations for the extended Schnakenberg model in Xie et al. (2021) except the different constants terms.

We summarize our results as follows,

Principal Result 1 *Let*

$$\tau = \frac{1}{\kappa} + \varepsilon^2 \hat{\tau},$$

and assume that $\hat{\tau} = O(1)$ *as* $\varepsilon \to 0$. *Then there exists a solution to the extended Gierer–Meinhardt system* (3.1) *consisting of* N *spikes nearly-uniformly spaced, but whose centers evolve near the symmetric configurations on a slow time-scale according to the following. Let* $\hat{x}_k$ *be the center of the* k*-th spike. Then* $\hat{x}_k \sim -1 + \frac{2k-1}{N} + \varepsilon p_k$ *where*

$$p_k = \sum_{j=1}^{N} Q_{kj} B_j(\varepsilon^2 t) \cos\left(\varepsilon \omega_j t + \theta_j(\varepsilon^2 t)\right). \tag{3.106}$$

In Eq. (3.106), Q_{kj} *is the entry of the matrix* Q *defined by Eq.* (2.10), ω_j *is defined by Eq.* (3.102) *and the associated amplitudes* $\{B_j(s),\ j = 1, \ldots, N\}$ *satisfy Eq.* (3.104).

3.3 Amplitude Equations for the Extended Gray–Scott Model

We consider the extended Gray–Scott system:

$$\begin{cases} u_t = \varepsilon^2 u_{xx} - (1-\kappa)u + Au^2 v - \kappa w, \\ 0 = Dv_{xx} + 1 - v - \frac{u^2 v}{\varepsilon}, \\ \tau w_t = u - w, \\ \text{Neumann boundary conditions at } x = \pm 1. \end{cases} \tag{3.107}$$

It has been shown in Kolokolnikov et al. (2005a) that there are two symmetric N-spike equilibrium solutions to the system (3.107) at $\tau = 0$ given asymptotically by

$$u_{\pm}(x) \sim \frac{1}{AV_{\pm}} \sum_{j=1}^{N} \rho(\varepsilon^{-1}(x - x_j)), \quad v_{\pm}(x) \sim 1 - \frac{1 - V_{\pm}}{c_g} \sum_{j=1}^{N} G(x, x_j), \tag{3.108}$$

where

$$V_{\pm} = \frac{1}{2}\left(1 \pm \sqrt{1 - 24 c_g / A^2}\right), \tag{3.109}$$

with $c_g := \left[2\sqrt{D} \tanh\left(\frac{1}{\sqrt{DN}}\right)\right]^{-1}$ defined in Eq. (3.76a). A necessary condition to have an N-spike solution is

$$c_g < \frac{A^2}{24}, \tag{3.110}$$

which implicitly poses a restriction on D. The stability analysis of these two symmetric N-spike equilibrium solutions of two-component system in Kolokolnikov et al. (2005a) further reveals that the solution contains V_+ is always unstable to the small eigenvalues when $N > 1$. As to the solution determined by V_-, we have the following lemma related to the stability of an N-spike equilibrium solution at $\tau = 0$, see Proposition 3.3 in Kolokolnikov et al. (2005a).

Lemma 2 *An N-spike equilibrium solution is stable at $\tau = 0$ if D satisfies the following transcendental equation*

$$D < \frac{4}{N^2 \ln^2\left(\frac{s_g+1}{s_g-1} + \sqrt{\left(\frac{s_g+1}{s_g-1}\right)^2 - 1}\right)}, \tag{3.111}$$

where

$$s_g := \frac{1 - V_-}{V_-}. \tag{3.112}$$

Now we start to derive the dynamics of spikes near the Hopf bifurcations. The inner region analysis of the Gray–Scott model is similar to the Schnakenberg model, while the outer solution has the same structure as the Gierer–Meinhardt model up to a constant addend. After a tedious but straightforward analysis as we have done for the extended Gierer–Meinhardt model, we obtain the following equations for the slow evolution of the amplitudes:

$$\frac{\mathrm{d}B_k}{\mathrm{d}t_2} = B_k\left[\frac{1}{2}(\hat{\tau}\kappa^2 + \beta_1\zeta_k) - \frac{3\beta_2}{8\kappa N}\sum_{j=1}^{N} a_{k,j}\omega_j^2 B_j^2\right], \tag{3.113a}$$

where

$$a_{k,j} = \begin{cases} N\sum_{l=1}^{N} Q_{lj}^4 & j = k \\ 2N\sum_{l=1}^{N} Q_{lj}^2 Q_{lk}^2 & j \neq k \end{cases}, \tag{3.113b}$$

and

$$\beta_1 := \frac{s_g\int_{-\infty}^{\infty}\rho^2\rho' y\,\mathrm{d}y}{c_g\int_{-\infty}^{\infty}\rho'^2\,\mathrm{d}y} = -\frac{2s_g}{c_g}, \quad \beta_2 := \frac{\int_{-\infty}^{\infty}(\rho'')^2\,\mathrm{d}y}{\int_{-\infty}^{\infty}\rho'^2\,\mathrm{d}y} = \frac{5}{7}, \quad \omega_k = \sqrt{-\kappa\beta_1\zeta_k}. \tag{3.113c}$$

The matrix Q is defined the same as Eq. (2.10), and $\zeta_k,\ k = 1, \ldots, N$ (with abuse of notations) are eigenvalues of

$$\mathcal{M} = \frac{c_g}{D}\mathcal{I} + \mathcal{G}_g + \frac{s_g}{c_g}\mathcal{P}\left(-\frac{s_g}{c_g}\mathcal{G} + \mathcal{I}\right)^{-1}\mathcal{P}^{\mathsf{T}}, \tag{3.114}$$

which can be computed as

$$\zeta_k = \frac{c_g}{D} - \frac{1}{D^{\frac{3}{2}}\nu_k} + \frac{s_g}{D^{\frac{3}{2}}\nu_k\left(c_g\sqrt{D}\nu_k - s_g\right)}\operatorname{csch}^2\left(\frac{2}{\sqrt{D}N}\right)\sin^2\left(\frac{\pi k}{N}\right). \tag{3.115}$$

Then, we arrive at the following result:

Principal Result 2 *Let*

$$\tau = \frac{1}{\kappa} + \varepsilon^2 \hat{\tau},$$

and assume that $\hat{\tau} = O(1)$ *as* $\varepsilon \to 0$. *Then there exists a solution to the extended Gray–Scott system* (3.107) *consisting of N spikes nearly-uniformly spaced, but whose centers evolve near the symmetric configurations on a slow time-scale according to the following. Let* $\hat{x}_k$ *be the center of the k-th spike. Then* $\hat{x}_k \sim -1 + \frac{2k-1}{N} + \varepsilon p_k$ *where*

$$p_k = \sum_{j=1}^{N} Q_{kj} B_j(\varepsilon^2 t) \cos\left(\varepsilon \omega_j t + \theta_j(\varepsilon^2 t)\right). \tag{3.116}$$

In Eq. (3.116), Q_{kj} *is the entry of the matrix Q defined by Eq.* (2.10), ω_j *is defined by* (3.113c) *and the associated amplitudes* $\{B_j(s),\ j = 1, \ldots, N\}$ *satisfy Eq.* (3.113a).

3.4 Numerical Validation

In this subsection we use finite element solver FlexPDE7 (Inc 2020) to numerically solve systems (3.1) and (3.107). In particular, we validate the reduced systems for the amplitude evolutions in the case of two spikes, as predicted in Principal Results 1 and 2. For the validation of N spikes' oscillatory dynamics, the readers are referred to Xie et al. (2021), where the authors have done various numerical computations to demonstrate the effectiveness of the reduced system for the Schnakenberg model.

We first outline our procedures. Initial two-spike equilibrium states for which we will use to test the dynamics are obtained by initializing a two-bump pattern in (3.1) and (3.107) with τ set well below the Hopf threshold $\frac{1}{\kappa}$. We then evolve (3.1) and (3.107) until the time t is sufficiently large that changes in solution are no longer observed. Using this equilibrium solution plus a perturbation $\left[0, 0, \alpha_1 \varepsilon^2 u_{cx}\left(\frac{x+0.5}{\varepsilon}\right) + \alpha_2 \varepsilon^2 u_{cx}\left(\frac{x-0.5}{\varepsilon}\right)\right]^{\mathsf{T}}$ as the initial condition, we increase τ to $\frac{1}{\kappa} + \hat{\tau}\varepsilon^2$ and try various values of α_1 and α_2 to test the sluggish dynamics of (3.104) and (3.113a) near the Hopf bifurcation. Here u_c denotes a single spike solution and $[\alpha_1, \alpha_2]$ gives the initial moving directions of two spikes.

Figure 2 and Fig. 3 illustrate the coexistence of in-phase and out-of-phase oscillations predicted by (3.104) and (3.113a). All parameters in the specific system are the same. In Fig. 2(a) and Fig 3(a), the initial perturbation is chosen as $[\alpha_1, \alpha_2] = [1, 1]$, resulting in-phase oscillations. In Fig. 2(b) and Fig 3(b), the initial perturbation is chosen as $[\alpha_1, \alpha_2] = [1, -1]$, resulting in out-of-phase oscillations. The evolution of the amplitudes described by (3.104) and (3.113a) are solved with MATLAB subroutine ODE45 and the results are in good agreement with the full PDE simulations.

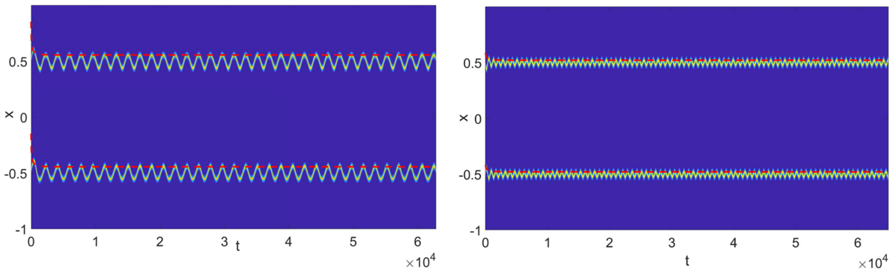

(a) In-phase oscillations.

(b) Out-of-phase oscillations.

Fig. 2 Two types of oscillations in GM model when τ is well beyond $\frac{1}{\kappa}$. The parameters are $\hat{\tau} = 300$, $\varepsilon = 0.01$, $D = \frac{0.2}{\ln^2(1+\sqrt{2})}$, $\kappa = 0.2$. The red dashed lines are the amplitudes' evolution obtained from solving the system (3.104). The only difference between Fig. 2(a) and Fig. 2(b) is the initial condition we select

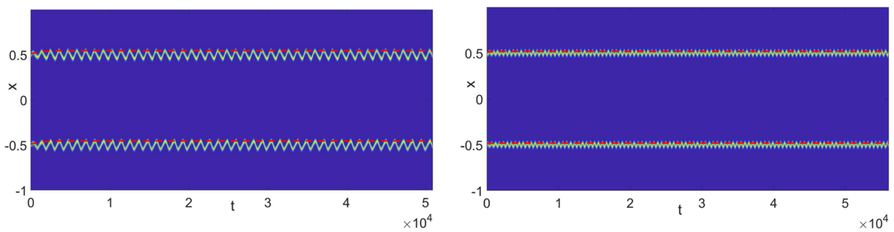

(a) In-phase oscillations.

(b) Out-of-phase oscillations.

Fig. 3 Two types of oscillations in GS model when τ is well beyond $\frac{1}{\kappa}$. The parameters are $\hat{\tau} = 450$, $\varepsilon = 0.01$, $D = 0.2$, $\kappa = 0.2$, $A = 6$. The red dashed lines are the amplitudes' evolution obtained from solving the system (3.113a). The difference between Fig. 3(a) and Fig. 3(b) is the initial conditions we select

4 Stability of Equilibria of the Amplitude Equations

In this section, we investigate the equilibrium points of the amplitude equations and their stability, which is crucial to understand the stable oscillations in the original reaction–diffusion systems. We start with the general form of amplitude equations

$$\frac{\mathrm{d}B_k}{\mathrm{d}t_2} = B_k\left[\frac{1}{2}(\hat{\tau}\kappa^2 + \beta_1\zeta_k) - \frac{3\beta_2}{8\kappa N}\sum_{j=1}^{N} a_{k,j}\omega_j^2 B_j^2\right], \tag{4.1}$$

We introduce new variable $X_k = \frac{3\beta_2}{8\kappa N} w_k^2 B_k^2$. Then, the system Eq. (4.1) is equivalent to

$$\frac{\mathrm{d}X_k}{\mathrm{d}t_2} = 2X_k(\tilde{\tau}_k - \sum_{j=1}^{N} a_{k,j}X_j), \text{ with } X_k \geq 0. \tag{4.2}$$

where $\tilde{\tau}_k = \frac{1}{2}(\hat{\tau}\kappa^2 + \beta_1\zeta_k)$. Note that $\tilde{\tau}_k$ is ranked in a descending order, namely, $\tilde{\tau}_1 > \tilde{\tau}_2 > \cdots > \tilde{\tau}_N$. In the following analysis, we will always assume $\tilde{\tau}_N > 0$ such that N Hopf modes are excited.

Denote $\mathcal{A}^{(N)}$ as the $N \times N$ matrix with entries $a_{k,j}$. In Appendix A, we calculate $a_{k,j}$ explicitly and have the following result:

Lemma 3 *For the matrix $\mathcal{A}^{(N)}$,*

- *when $N = 2n + 1$, we have*

$$a_{k,j} = \begin{cases} 1, & k = j = N, \\ \frac{3}{2}, & k = j \neq N, \\ 1, & k + j = N, \\ 2, & else. \end{cases} \qquad \det \mathcal{A}^{(N)} = \frac{8n+3}{3}\left(-\frac{3}{4}\right)^n, \tag{4.3}$$

- *when $N = 2n$, we have*

$$a_{k,j} = \begin{cases} 1, & k = j = N \ \ and \ \ k = j = n, \\ \frac{3}{2}, & k = j \neq N \ \ and \ \ k = j \neq n, \\ 1, & k + j = N, \\ 2, & else. \end{cases} \qquad \det \mathcal{A}^{(N)} = -\frac{8n+1}{3}\left(-\frac{3}{4}\right)^{n-1}. \tag{4.4}$$

For concreteness, when $N = 5$ and $N = 6$, we have

$$\mathcal{A}^{(5)} = \begin{pmatrix} \frac{3}{2} & 2 & 2 & 1 & 2 \\ 2 & \frac{3}{2} & 1 & 2 & 2 \\ 2 & 1 & \frac{3}{2} & 2 & 2 \\ 1 & 2 & 2 & \frac{3}{2} & 2 \\ 2 & 2 & 2 & 2 & 1 \end{pmatrix}, \quad \mathcal{A}^{(6)} = \begin{pmatrix} \frac{3}{2} & 2 & 2 & 2 & 1 & 2 \\ 2 & \frac{3}{2} & 2 & 1 & 2 & 2 \\ 2 & 2 & 1 & 2 & 2 & 2 \\ 2 & 1 & 2 & \frac{3}{2} & 2 & 2 \\ 1 & 2 & 2 & 2 & \frac{3}{2} & 2 \\ 2 & 2 & 2 & 2 & 2 & 1 \end{pmatrix}. \tag{4.5}$$

The equilibrium points of the system Eq. (4.2) can be obtained by setting the left-hand side to be 0, i.e.,

$$X_k(\tilde{\tau}_k - \sum_{j=1}^{N} a_{k,j} X_j) = 0, \ \ X_k \geq 0, \ \ \text{for } k = 1, \cdots, N. \tag{4.6}$$

We denote S as a subset of the set $S_N = \{1, \cdots, N\}$ with m entries and $\bar{S}$ to be the complement set of S. The equilibrium points satisfy $\boldsymbol{X}_S = 0$ and $\mathcal{A}_{\bar{S}}^{(N)} \boldsymbol{X}_{\bar{S}} = \tilde{\boldsymbol{\tau}}_{\bar{S}}$, where $\mathcal{A}_{\bar{S}}^{(N)}$ is the square submatrix obtained by removing all the columns and rows with index in the set S from $\mathcal{A}^{(N)}$. For instance, when $S = \{1, 4\}$, the submatrix $\mathcal{A}_{\bar{S}}^{(N)}$ is defined as a new matrix obtained by removing the first and fourth columns and the first and fourth rows from $\mathcal{A}^{(N)}$,

$$\mathcal{A}_{\bar{S}}^{(5)} = \begin{pmatrix} \frac{3}{2} & 1 & 2 \\ 1 & \frac{3}{2} & 2 \\ 2 & 2 & 1 \end{pmatrix}, \quad \mathcal{A}_{\bar{S}}^{(6)} = \begin{pmatrix} \frac{3}{2} & 2 & 2 & 2 \\ 2 & 1 & 2 & 2 \\ 2 & 2 & \frac{3}{2} & 2 \\ 2 & 2 & 2 & 1 \end{pmatrix}. \tag{4.7}$$

If $\mathcal{A}_{\bar{S}}^{(N)}$ is invertible for all S with $m = 1, \cdots, N$, we can at most find 2^N non-negative solutions to Eq. (4.6).

Remark 6 For a given S, we show that $\mathcal{A}_{\bar{S}}$ is invertible in Appendix A. Thus there exists a solution to the system $\mathcal{A}_{\bar{S}}^{(N)} X_{\bar{S}} = \tilde{\boldsymbol{\tau}}_{\bar{S}}$. However, the solution may be negative unless we impose suitable conditions on $\tilde{\boldsymbol{\tau}}_{\bar{S}}$.

For succinctness, we will represent $\mathcal{A}^{(N)}$ by $\mathcal{A}$ in the remainder of this section. Linearizing the ODE system Eq. (4.2) around a equilibrium point $\mathbf{X} = [X_1, X_2, \cdots, X_N]^\mathsf{T}$ leads to the following eigenvalue problem:

$$\lambda \phi_k = 2\left(\tilde{\tau}_k - \sum_{j=1}^{N} a_{k,j} X_j\right)\phi_k - 2X_k \sum_{j=1}^{N} a_{k,j}\phi_j, \quad 1 \le k \le N. \tag{4.8}$$

For the equilibrium point satisfying $\boldsymbol{X}_S = 0$ and $\boldsymbol{X}_{\bar{S}} = \mathcal{A}_{\bar{S}}^{-1}\tilde{\boldsymbol{\tau}}_{\bar{S}} > 0$, the eigenvalue problem can be decomposed into two sets of equations:

$$\lambda \phi_k = -2X_k \sum_{j\in\bar{S}} a_{k,j}\phi_j, \quad k \in \bar{S}, \tag{4.9a}$$

$$\lambda \phi_k = 2\left(\tilde{\tau}_k - \sum_{j\in\bar{S}} a_{k,j} X_j\right)\phi_k, \quad k \in S. \tag{4.9b}$$

After relabeling, we write Eq. (4.9) in a matrix form

$$\lambda \boldsymbol{\phi} = 2\begin{pmatrix} -\mathcal{D}_{X_{\bar{S}}}\mathcal{A}_{\bar{S}} & O_{N-m,m} \\ O_{m,N-m} & D_{\tilde{\tau}} \end{pmatrix}\boldsymbol{\phi}, \tag{4.10}$$

where $\mathcal{D}_{\boldsymbol{X}_{\bar{S}}}$ is a diagonal matrix with $\boldsymbol{X}_{\bar{S}}$ on its diagonal, $O_{*,*}$ is a zero matrix and $D_{\tilde{\tau}} = \mathrm{diag}(\mathbf{d}_{\tilde{\tau}})$ is a $m \times m$ diagonal matrix with $\mathbf{d}_{\tilde{\tau}} = [\tilde{\tau}_m - \sum_{j\in\bar{S}} a_{m,j}X_j]$ for $m \in S$. Thus, an eigenvalue of $-\mathcal{D}_{X_{\bar{S}}}\mathcal{A}_{\bar{S}}$ is also an eigenvalue of Eq. (4.8). We will use this fact to rule out a large part of the unstable equilibrium points. A key observation is the following lemma.

Lemma 4 *For the equilibrium point satisfying $\boldsymbol{X}_S = 0$ and $\boldsymbol{X}_{\bar{S}} = \mathcal{A}_{\bar{S}}^{-1}\tilde{\boldsymbol{\tau}}_{\bar{S}}$, if the matrix $\mathcal{A}_{\bar{S}}$ has a negative eigenvalue, then the equilibrium point is unstable.*

Proof It suffices to show that the matrix $-\mathcal{D}_{\boldsymbol{X}_{\bar{S}}}\mathcal{A}_{\bar{S}}$ has a positive eigenvalue when $\mathcal{A}_{\bar{S}}$ has a negative eigenvalue. A direct computation yields $\mathcal{D}_{\boldsymbol{X}_{\bar{S}}}\mathcal{A}_{\bar{S}}$ is similar to the matrix $\mathcal{D}^{\frac{1}{2}}_{\boldsymbol{X}_{\bar{S}}}\mathcal{A}_{\bar{S}}\mathcal{D}^{\frac{1}{2}}_{\boldsymbol{X}_{\bar{S}}}$, which is congruent to the matrix $\mathcal{A}_{\bar{S}}$.

By Sylvester's law of inertia, the matrix $\mathcal{D}^{\frac{1}{2}}_{\boldsymbol{X}_{\bar{S}}}\mathcal{A}_{\bar{S}}\mathcal{D}^{\frac{1}{2}}_{\boldsymbol{X}_{\bar{S}}}$ and the matrix $\mathcal{A}_{\bar{S}}$ have the same number of positive, negative and zero eigenvalues. Thus, if $\mathcal{A}_{\bar{S}}$ has a negative eigenvalue, then $-\mathcal{D}_{\boldsymbol{X}_{\bar{S}}}\mathcal{A}_{\bar{S}}$ has a positive eigenvalue. □

Denote $\#S$ as the cardinality of the set S. Regarding the eigenvalues of $\mathcal{A}_{\bar{S}}$, we have the following results:

Lemma 5 *When $\#\bar{S} > 2$, the matrix $\mathcal{A}_{\bar{S}}$ has at least one negative eigenvalue.*

Proof To prove $\mathcal{A}_{\bar{S}}$ has at least one negative eigenvalue, it suffices to show that $\mathcal{A}_{\bar{S}}$ is not positive semi-definite. Let $a_{k,j}$ be the entry of $\mathcal{A}_{\bar{S}}$. When $\#\bar{S} > 2$, there exists an index k such that $a_{k+1,k} = a_{k,k+1} = 2$. We choose $x = [0, \cdots, \overbrace{1}^{k}, -1, \cdots, 0]^{\mathsf{T}}$, then $x^{\mathsf{T}}\mathcal{A}_{\bar{S}}x = a_{k,k} - a_{k+1,k} - a_{k,k+1} + a_{k+1,k+1}$. As the entries $a_{k,k}$ and $a_{k+1,k+1}$ are either $\frac{3}{2}$ or 1, we have $x^{\mathsf{T}}\mathcal{A}_{\bar{S}}x = -1, -2$, or $-\frac{3}{2}$. By Sylvester's criterion, $\mathcal{A}_{\bar{S}}$ is not positive semi-definite. Thus, $\mathcal{A}_{\bar{S}}$ has at least one negative eigenvalue. □

Lemma 6 *When $\#\bar{S} = 2$, except the matrix*

$$\mathcal{A}_{\bar{S}} = \begin{pmatrix} \frac{3}{2} & 1 \\ 1 & \frac{3}{2} \end{pmatrix}, \tag{4.11}$$

the matrix $A_{\bar{S}}$ has at least one negative eigenvalue.

Proof When $\#\bar{S} = 2$, the matrix $A_{\bar{S}}$ has the following possible forms:

$$\mathcal{A}_{\bar{S}} = \begin{pmatrix} \frac{3}{2} & 1 \\ 1 & \frac{3}{2} \end{pmatrix}, \quad \begin{pmatrix} \frac{3}{2} & 2 \\ 2 & \frac{3}{2} \end{pmatrix}, \quad \text{or } \begin{pmatrix} \frac{3}{2} & 2 \\ 2 & 1 \end{pmatrix}, \quad \text{for } N \text{ is odd}, \tag{4.12}$$

$$\mathcal{A}_{\bar{S}} = \begin{pmatrix} \frac{3}{2} & 1 \\ 1 & \frac{3}{2} \end{pmatrix}, \quad \begin{pmatrix} \frac{3}{2} & 2 \\ 2 & \frac{3}{2} \end{pmatrix}, \quad \begin{pmatrix} \frac{3}{2} & 2 \\ 2 & 1 \end{pmatrix}, \quad \text{or } \begin{pmatrix} 1 & 2 \\ 2 & 1 \end{pmatrix} \quad \text{for } N \text{ is even}. \tag{4.13}$$

We can easily calculate their eigenvalues explicitly and find that only the eigenvalues of $\mathcal{A}_{\bar{S}} = \begin{pmatrix} \frac{3}{2} & 1 \\ 1 & \frac{3}{2} \end{pmatrix}$ are all positive. □

The above two lemmas have identified most of the unstable equilibrium points. Next, we examine the stability of the remaining equilibrium points.

Lemma 7 *For $\#\bar{S} = 1$ and $\tilde{\tau}_N > \frac{2}{3}\tilde{\tau}_1$,*

- *when N is odd, only the equilibrium point $\boldsymbol{X} = [0, \cdots, 0, \tilde{\tau}_N]^{\mathsf{T}}$ is stable;*
- *when N is even, only the equilibrium points $\boldsymbol{X} = [0, \cdots, \tilde{\tau}_{N/2}, \cdots, 0]^{\mathsf{T}}$ and $\boldsymbol{X} = [0, \cdots, 0, \tilde{\tau}_N]^{\mathsf{T}}$ are stable.*

Proof For the equilibrium point $\mathbf{X} = [0, \cdots, \frac{\tilde{\tau}_k}{a_{k,k}}, \cdots, 0]^{\mathsf{T}}$, the eigenvalue problem Eq. (4.8) can be written in the following matrix form

$$\lambda\boldsymbol{\phi} = 2\mathcal{D}_{\tilde{\tau}}\boldsymbol{\phi}, \tag{4.14}$$

where $\mathcal{D}_{\tilde{\tau}} = \mathrm{diag}(\mathbf{d})$ is a diagonal matrix with $\mathbf{d} = [\tilde{\tau}_1 - \dfrac{a_{1,k}}{a_{k,k}}\tilde{\tau}_k, \tilde{\tau}_2 - \dfrac{a_{2,k}}{a_{k,k}}\tilde{\tau}_k, \cdots, -\tilde{\tau}_k, \tilde{\tau}_{k+1} - \dfrac{a_{k+1,k}}{a_{k,k}}\tilde{\tau}_k, \cdots, \tilde{\tau}_N - \dfrac{a_{N,k}}{a_{k,k}}\tilde{\tau}_k]$. Hence, the equilibrium point is unstable if one entry in $\mathbf{d}$ is positive.

- When N is odd, the $(N-k)$-th entry of $\mathbf{d}$ is

$$\tilde{\tau}_{N-k} - \frac{a_{N-k,k}}{a_{k,k}}\tilde{\tau}_k = \tilde{\tau}_{N-k} - \frac{2}{3}\tilde{\tau}_k > \tilde{\tau}_N - \frac{2}{3}\tilde{\tau}_1 > 0, \text{ for } k \neq N. \tag{4.15}$$

  Thus, the equilibrium point $\mathbf{X} = [0, \cdots, \frac{\tilde{\tau}_k}{a_{k,k}}, \cdots, 0]^\mathsf{T}$ is unstable for $k \neq N$. Whereas for $k = N$, we have $\lambda_{\max} = 2(\tilde{\tau}_1 - 2\tilde{\tau}_N) < 0$. Therefore, only the equilibrium point $\mathbf{X} = [0, \cdots, 0, \tilde{\tau}_N]^\mathsf{T}$ is stable.
- When N is even, with a similar analysis as done for the odd case, we can show that only the equilibrium points $\boldsymbol{X} = [0, \cdots, \tilde{\tau}_{N/2}, \cdots, 0]^\mathsf{T}$ and $\boldsymbol{X} = [0, \cdots, 0, \tilde{\tau}_N]^\mathsf{T}$ are stable. □

Lemma 8 *For* $\#\bar{S} = 2$ *and* $\tilde{\tau}_N > \frac{2}{3}\tilde{\tau}_1$,

- *when N is odd, the stable equilibrium points are* $[0, \cdots, X_k, 0, \cdots, X_{N-k}, \cdots, 0]^\mathsf{T}$ *for* $k = 1, \cdots, \frac{N-1}{2}$, *where* X_k*and* X_{N-k} *satisfy:*

$$\begin{pmatrix} \frac{3}{2} & 1 \\ 1 & \frac{3}{2} \end{pmatrix} \begin{pmatrix} X_k \\ X_{N-k} \end{pmatrix} = \begin{pmatrix} \tilde{\tau}_k \\ \tilde{\tau}_{N-k} \end{pmatrix}; \tag{4.16}$$

- *when N is even, the stable equilibrium points are* $[0, \cdots, X_k, 0, \cdots, X_{N-k}, \cdots, 0]^\mathsf{T}$ *for* $k = 1, \cdots, \frac{N}{2} - 1$, *where* X_k *and* X_{N-k} *satisfy:*

$$\begin{pmatrix} \frac{3}{2} & 1 \\ 1 & \frac{3}{2} \end{pmatrix} \begin{pmatrix} X_k \\ X_{N-k} \end{pmatrix} = \begin{pmatrix} \tilde{\tau}_k \\ \tilde{\tau}_{N-k} \end{pmatrix}. \tag{4.17}$$

Proof For compactness, we only prove the case when N is odd. Solving Eq. (4.16) yields

$$[X_k, X_{N-k}] = [\frac{6}{5}\tilde{\tau}_k - \frac{4}{5}\tilde{\tau}_{N-k}, -\frac{4}{5}\tilde{\tau}_k + \frac{6}{5}\tilde{\tau}_{N-k}], \tag{4.18}$$

which is positive under the condition that $\tilde{\tau}_N > \frac{2}{3}\tilde{\tau}_1$. The eigenvalue problem Eq. (4.10) becomes

$$\lambda\boldsymbol{\phi} = 2\begin{pmatrix} B & O \\ O & D_{\tilde{\tau}} \end{pmatrix}\boldsymbol{\phi}, \tag{4.19}$$

where $D_{\tilde{\tau}} = \mathrm{diag}(\mathbf{d}_{\tilde{\tau}})$ is a $(N-2)\times(N-2)$ diagonal matrix with $\mathbf{d}_{\tilde{\tau}} = [\tilde{\tau}_m - a_{m,k}X_k - a_{m,N-k}X_{N-k}]$ for $m \neq k, N-k$ and B is a 2×2 matrix defined by

$$B = -\begin{pmatrix} X_k & 0 \\ 0 & X_{N-k} \end{pmatrix}\begin{pmatrix} \frac{3}{2} & 1 \\ 1 & \frac{3}{2} \end{pmatrix}. \tag{4.20}$$

The eigenvalue of B is negative, thus we only need to examine the entry of $\mathbf{d}_{\tilde{\tau}}$. When $\tilde{\tau}_N > \frac{2}{3}\tilde{\tau}_1$, we have

$$\tilde{\tau}_m - a_{m,k}X_k - a_{m,N-k}X_{N-k} = \tilde{\tau}_m - \frac{4}{5}(\tilde{\tau}_k + \tilde{\tau}_{N-k}) < \tilde{\tau}_1 - \frac{8}{5}\tilde{\tau}_N < -\frac{1}{10}\tilde{\tau}_N < 0. \tag{4.21}$$

Therefore, the equilibrium points $[0, \cdots, X_k, 0, \cdots, X_{N-k}, \cdots, 0]$ for $k = 1, \cdots, \frac{N-1}{2}$ are stable. □

We summarize all the above lemmas and obtain our main results.

Proposition 1 *When $\tilde{\tau}_N > \frac{2\tilde{\tau}_1}{3}$, the system Eq. (4.2) possesses $\lfloor N/2 \rfloor + 1$ stable equilibrium points.*

Proposition 1 implies that we can observe at most $\lfloor N/2 \rfloor + 1$ stable oscillatory patterns when $\tilde{\tau}$ is above a certain value.

Remark 7 When $\hat{\tau}$ is big enough, the stability of the oscillatory patterns is determined by the direction vectors $\left\{\boldsymbol{q}_1, \boldsymbol{q}_2, \cdots, \boldsymbol{q}_N\right\}$ that are independent of the spike profile. As the direction vectors are the same for these three singular-perturbed systems, Proposition 1 is valid for all of them.

5 Discussion

Temporal oscillations in the pattern position are wildly reported in three-component systems (Gurevich et al. 2006; Giunta et al. 2021). For a two-component system that admits stable stationary localized patterns, a simple way of producing traveling patterns is to add a non-diffusive inhabitant to the activator of the two-components systems and increase the reaction-ratio of that inhabitant (Or-Guil et al. 1998). In Xie et al. (2021), by introducing a second inhibitor to the Schnakenberg model, the coexistence of multiple oscillating patterns is reported and analyzed. However, the number of stable periodic oscillations for an N-spike solution is still unknown. In this article, we extended the analysis to extensions of two other well-known systems the Gierer–Meinhardt system and the Gray–Scot system. Moreover, we rigorously prove, based on the long-time evolution of the amplitudes of the oscillations, that there are at most $\lfloor N/2 \rfloor + 1$ stable patterns for three-component extensions of these systems, thereby resolving the open problem. Our findings shed light on the initiation of rich dynamical behaviors of localized structures. It is worthwhile to note that our analysis is only valid for the bifurcation parameter at an $\mathcal{O}(\varepsilon^2)$ distance to the thresholds. More complex oscillatory patterns, such as zigzag oscillation, when τ exceeds τ_c in an $\mathcal{O}(\varepsilon)$ or $\mathcal{O}(1)$ scale are beyond the scope of this article and need alternative treatments.

As described in Appendix B, the system we consider is a simplified version of the following system

$$\begin{cases} u_t = \varepsilon^2 u_{xx} + f(u, v) - \kappa w \\ \tau_v v_t = D_v v_{xx} + g(u, v) & x \in (-1, 1), \quad t \geq 0, \\ \tau_w w_t = D_w w_{xx} + cu - w \\ \text{Neumann boundary conditions for at } x = \pm 1. \end{cases} \tag{5.1}$$

To facilitate the analysis, we have assumed that τ_v and D_w are sufficiently small and can be set to zero. We remark that this assumption leads to a singular reduction of the system since it alters the order of differential equation. The generalizability of the conclusions drawn in this paper to the case where τ_v and D_w are small but not zero remains uncertain. Some investigation has been conducted in Saadi et al. (2024) using a three-component Brusselator model with $D_w = \varepsilon^4$, revealing the persistence of spike patterns even with nonzero D_w. Conversely, in the absence of the third component, it is widely acknowledged that increasing τ_v sufficiently results in oscillations in spike height, as demonstrated in Ward and Wei (2003a, b). We expect to see a combination of jumping and oscillating spikes in some parameter regimes.

The new phenomena we observe are not limited to the systems we have studied. In a more realistic situation with more complicated reaction terms and additional diffusion of component w, e.g.

$$\begin{cases} u_t = \varepsilon^2 u_{xx} + f(u, v) - \kappa u w, \\ \tau_v v_t = D_v v_{xx} + g(u, v), & x \in (-1, 1)\,, \quad t \geq 0. \\ \tau_w w_t = D_w \varepsilon^2 w_{xx} + \kappa u w - w, \\ \text{Neumann boundary conditions at } x = \pm 1. \end{cases} \tag{5.2}$$

we also observe multiple stable oscillatory moving spikes with suitable parameters. Although the localized profiles of u and w now are unknown analytically, a similar analysis can be done since the localized components, u and w, do not change the stability analysis of the oscillations.

Our result is applicable to the system with a uniform feed rate or precursor. It would be interesting to investigate how the heterogeneity impacts the stability threshold as well as the spike dynamics at the onset, which are more biologically relevant because they model the hierarchical formation of small-scale structures induced by large-scale inhomogeneity. Many results exist for two-component systems with heterogeneity. For example, the existence of a solution consisting of a cluster of N spikes near a non-degenerate local minimum point of the smooth inhomogeneity in GM model has been rigorously shown in 1-D (Wei and Winter 2017) and 2-D (Wei et al. 2017) domains. The evolution of multi-pulse patterns in an extended Gray–Scott–Klausmeier equation with parameters that change in time and/or space is investigated in Bastiaansen and Doelman (2019). One future direction is to explore the stability and evolution of these spike clusters in three-component systems.

For the extended Gierer–Meinhardt system (3.1) with periodic boundary condition, numerical simulations exhibit a traveling and breathing two-spike pattern, which is similar to the moving and breathing solitons discussed in Gurevich and Friedrich (2013). It is unclear whether such behaviors are due to the same mechanism, i.e., the excitation of both drift and Hopf modes.

More complex dynamics are expected in 2-D domains, the freedom in different directions and impact of the domain geometry on the instability remain to be investigated. For example, Xie and Kolokolnikov (2017) and Tzou and Xie (2023) employ a hybrid asymptotic-numerical method to investigate the Hopf bifurcation related to translational instabilities for the Schnakenberg model with the high feed rate in two-dimensional domains. Various domains and spot arrangements are numerically tested there, exhibiting rich dynamics. It is an open question to explore these effects on the dynamics of multiple spikes in our extended three-component systems.

Appendix A. Calculations of $\mathcal{A}$ and $\mathcal{A}_{\bar{S}}$

We prove Lemma 3

Proof First, we calculate all entries of the matrix $\mathcal{A}$.

Now we calculate the entries on the diagonal of the matrix $\mathcal{A}$, it is easy to find $a_{N,N} = 1$. When $N = 2n + 1$, for $j = 1, \ldots, N - 1$, we have

$$a_{j,j} = N \sum_{l=1}^{N} Q_{l,j}^4 = \frac{4}{N} \sum_{l=1}^{N} \sin^4 \frac{(2l-1)j\pi}{2N} = \frac{4}{N} \left(\frac{3N}{8} + \frac{\sin(4j\pi)}{16 \sin \frac{2j\pi}{N}} - \frac{\sin(2j\pi)}{4 \sin \frac{j\pi}{N}} \right) = \frac{3}{2}. \tag{A.1}$$

When $N = 2n$, $a_{j,j} = \frac{3}{2}$ for $j \neq n,\ N$. For $j = n$, we have

$$a_{n,n} = N \sum_{l=1}^{N} Q_{l,n}^4 = \frac{4}{N} \sum_{l=1}^{N} \sin^4 \frac{(2l-1)\pi}{4} = \frac{4}{N} \left(\frac{3N}{8} + \frac{1}{8} \sum_{l=1}^{N} \cos(2l-1)\pi \right) = 1. \tag{A.2}$$

Here we use the formula

$$\sin^4 x = \frac{3}{8} + \frac{1}{8}\cos(4x) - \frac{1}{2}\cos(2x), \quad \sum_{k=1}^{N} \cos(2k-1)x = \frac{\sin(2Nx)}{2\sin x}, \\ x \neq k\pi \ (k \in \mathbf{N}^+). \tag{A.3}$$

Next, we calculate the other entries of the matrix $\mathcal{A}$. For $i \neq j$ $(i = 1, \cdots, N - 1,\ j = 1, \cdots, N-1)$ and $i + j \neq N$, we have

$$
\begin{aligned}
a_{i,j} &= \frac{8}{N}\sum_{l=1}^{N}\sin^2\frac{(2l-1)i\pi}{2N}\sin^2\frac{(2l-1)j\pi}{2N} \\
&= \frac{1}{N}\sum_{l=1}^{N}\Bigg[\left(\cos\frac{(2l-1)(i+j)\pi}{N}+\cos\frac{(2l-1)(j-i)\pi}{N}\right) \\
&\quad -2\left(\cos\frac{(2l-1)i\pi}{N}+\cos\frac{(2l-1)j\pi}{N}\right)\Bigg]+2 \\
&= \frac{1}{N}\left(\frac{\sin(2(i+j)\pi)}{2\sin\frac{(i+j)\pi}{N}}+\frac{\sin(2(j-i)\pi)}{2\sin\frac{(j-i)\pi}{N}}\right)-\frac{2}{N}\left(\frac{\sin(2i\pi)}{2\sin\frac{i\pi}{N}}+\frac{\sin(2j\pi)}{2\sin\frac{j\pi}{N}}\right)+2 \\
&= 2.
\end{aligned}
\tag{A.4}
$$

For $i+j=N$, we have

$$
\begin{aligned}
a_{i,j} &= \frac{8}{N}\sum_{l=1}^{N}\sin^2\frac{(2l-1)i\pi}{2N}\sin^2\frac{(2l-1)j\pi}{2N} \\
&= \frac{1}{N}\Bigg[\sum_{l=1}^{N}\left(\cos(2l-1)\pi+\cos\frac{(2l-1)(j-i)\pi}{N}\right) \\
&\quad -2\left(\cos\frac{(2l-1)i\pi}{N}+\cos\frac{(2l-1)j\pi}{N}\right)\Bigg]+2 \\
&= \frac{1}{N}\left(-N+\frac{\sin(2(j-i)\pi)}{2\sin\frac{(j-i)\pi}{N}}\right)-\frac{2}{N}\left(\frac{\sin(2i\pi)}{2\sin\frac{i\pi}{N}}+\frac{\sin(2j\pi)}{2\sin\frac{j\pi}{N}}\right)+2 \\
&= 1.
\end{aligned}
\tag{A.5}
$$

For $i=1,\cdots,N-1$, we have

$$
\begin{aligned}
a_{N,i} = a_{i,N} &= \frac{4}{N}\sum_{l=1}^{N}\sin^2\frac{(2l-1)i\pi}{2N} = 2-\frac{2}{N}\sum_{l=1}^{N}\cos\frac{(2l-1)i\pi}{N} \\
&= 2-\frac{2}{N}\frac{\sin(2i\pi)}{2\sin\frac{i\pi}{N}} = 2.
\end{aligned}
\tag{A.6}
$$

Finally, we compute the determinant of $\mathcal{A}$. We first define the matrix $B_{(2n)\times(2n)}$ as

$$
B_{(2n)\times(2n)} = \begin{pmatrix} -\frac{1}{2} & 0 & \cdots & 0 & -1 \\ 0 & -\frac{1}{2} & \cdots & -1 & 0 \\ \vdots & \vdots & \ddots & \vdots & \vdots \\ 0 & -1 & \cdots & -\frac{1}{2} & 0 \\ -1 & 0 & \cdots & 0 & -\frac{1}{2} \end{pmatrix}.
\tag{A.7}
$$

Using some elementary transformations, we obtain

$$\det(\mathcal{A})\begin{cases}\xlongequal[r_N+\frac{4}{3}r_i,\ i=1,\cdots,N-1]{r_j-r_N,\ j=1,\cdots,N-1}\left(1+\frac{8n}{3}\right)\det(B_{(2n)\times(2n)})=\left(1+\frac{8n}{3}\right)\times\left(-\frac{3}{4}\right)^n, & \text{for } N=2n+1,\\ \xlongequal[r_N+\frac{4}{3}r_i,\ i\neq n,N,\ r_N+2r_n]{r_j-r_N,\ j=1,\cdots,N-1}-\left(\frac{1}{3}+\frac{8n}{3}\right)\det(B_{(2n-2)\times(2n-2)})=-\left(\frac{1}{3}+\frac{8n}{3}\right)\times\left(-\frac{3}{4}\right)^{n-1}, & \text{for } N=2n.\end{cases}$$

□

Then we show that $\mathcal{A}_{\bar{S}}$ is invertible.

Recall that S is a subset of the set $S_N=\{1,\cdots,N\}$ with m elements, and $\bar{S}$ is the complement of S. $\mathcal{A}_{\bar{S}}$ is the square submatrix obtained by removing all the columns and rows with index in the set S. We shall discuss two cases according to the parity of N. In the following we shall only give details for the case where N is even, the odd case is simpler and we will omit the details.

1. When $N=2n$, according to whether n and $2n$ belong to S, it will be divided into four cases.

(1). If $\#S=m$ and $n,\ 2n\in S$, by elementary transformation that exchanges any two rows and corresponding two columns, the original matrix $\mathcal{A}_{\bar{S}}$ can be transformed into the following one

$$\begin{pmatrix} C_{s\times s}(a) & E^{\mathsf{T}}_{t\times s}\\ E_{t\times s} & D_{t\times t}\end{pmatrix}, \tag{A.8}$$

where $s=2n-2m+3$, $t=m-3$, $a=\frac{3}{2}$ and matrices C, D, E are as follows

$$C_{s\times s}(a)=\begin{pmatrix}\frac{3}{2} & 2 & \cdots & 2 & 1 & 2\\ 2 & \frac{3}{2} & \cdots & 1 & 2 & 2\\ \vdots & \vdots & \ddots & \vdots & \vdots & \vdots\\ 2 & 1 & \cdots & \frac{3}{2} & 2 & 2\\ 1 & 2 & \cdots & 2 & \frac{3}{2} & 2\\ 2 & 2 & \cdots & 2 & 2 & a\end{pmatrix},\quad D_{t\times t}=\begin{pmatrix}\frac{3}{2} & 2 & \cdots & 2\\ 2 & \frac{3}{2} & \cdots & 2\\ \vdots & \vdots & \ddots & \vdots\\ 2 & 2 & \cdots & \frac{3}{2}\end{pmatrix},\quad E_{t\times s}=\begin{pmatrix}2 & 2 & \cdots & 2\\ 2 & 2 & \cdots & 2\\ \vdots & \vdots & \ddots & \vdots\\ 2 & 2 & \cdots & 2\end{pmatrix}. \tag{A.9}$$

Let r_j and c_i represent j-th row and i-th column, respectively. Using some elementary transformations, we have

$$\begin{pmatrix} C_{s\times s}(a) & E^{\mathsf{T}}_{t\times s}\\ E_{t\times s} & D_{t\times t}\end{pmatrix}\xlongequal[\substack{r_{2n-2m+3}+\frac{1}{m-2}r_{2n-2m+3+j},\ j=1,\cdots,m-3\\ c_{2n-2m+3}+\frac{1}{m-2}c_{2n-2m+3+j},\ j=1,\cdots,m-3}]{\substack{r_{2n-2m+3+j}-r_{2n-2m+3},\ j=1,\cdots,m-3\\ c_{2n-2m+3+j}-c_{2n-2m+3},\ j=1,\cdots,m-3}}\begin{pmatrix} C_{s_1\times s_1}(a_1) & O^{\mathsf{T}}_{t_1\times s_1}\\ O_{t_1\times s_1} & F_{t_1\times t_1}\end{pmatrix}.$$

where $s_1=2n-2m+3$, $t_1=m-3$, $a_1=2-\frac{1}{2(m-2)}$, $O_{t_1\times s_1}$ is a zero matrix and matrix F is as follows

$$F_{t_1\times t_1}=\begin{pmatrix}-1 & -\frac{1}{2} & \cdots & -\frac{1}{2}\\ -\frac{1}{2} & -1 & \cdots & -\frac{1}{2}\\ \vdots & \vdots & \ddots & \vdots\\ -\frac{1}{2} & -\frac{1}{2} & \cdots & -1\end{pmatrix}. \tag{A.10}$$

Here r_i-r_j means -1 times the j-th row of the matrix is added to the i-th row of the matrix, c_k-c_l means -1 times the l-th column of matrix is added to the i-th column of the matrix. Using the similar method to calculating the determinant of $\mathcal{A}$, we have

$$\det(C_{s\times s}) = \begin{cases} \left(\frac{8s-8}{3} + a\frac{-4s+7}{3}\right) \times \left(-\frac{3}{4}\right)^{\frac{s-1}{2}}, & \text{for } s \text{ is odd,} \\ -\left(\frac{8s-4}{3} + a\frac{-4s+5}{3}\right) \times \left(-\frac{3}{4}\right)^{\frac{s-2}{2}}, & \text{for } s \text{ is even.} \end{cases} \tag{A.11}$$

and

$$\det\left(F_{t\times t}\right) \xlongequal[r_j-\frac{1}{t+1}r_1,\ j=2,\cdots,t]{r_1+r_j,\ j=2,\cdots,t} \left(-\frac{1}{2}\right)^t \times (t+1) \tag{A.12}$$

Therefore we have

$$\left|\det(\mathcal{A}_{\bar{S}})\right| = \left|\frac{4n}{3} + \frac{2m}{3} - \frac{19}{6}\right| \times \left(\frac{3}{4}\right)^{n-m+1} \times \left(\frac{1}{2}\right)^{m-3}.$$

(2). If $\#S = m$ and $n,\ 2n \notin S$, by elementary transformation that exchanges any two rows and corresponding two columns, the original matrix $\mathcal{A}_{\bar{S}}$ can be transformed into (A.8), where $s = 2n - 2m$, $t = m$, $a = 1$. Again using elementary transformations, we have

$$\begin{pmatrix} C_{s\times s}(a) & E^{\mathsf{T}}_{t\times s} \\ E_{t\times s} & D_{t\times t} \end{pmatrix} \xlongequal[\substack{r_{2n-2m+1}-r_{2n-2m},\ c_{2n-2m+1}-c_{2n-2m} \\ r_{2n-2m}+\frac{2m}{2m+1}r_{2n-2m+1},\ c_{2n-2m}+\frac{2m}{2m+1}c_{2n-2m+1}}]{\substack{r_{2n-2m+1+j}-r_{2n-2m+1},\ j=1,\cdots,m-1 \\ c_{2n-2m+1+j}-c_{2n-2m+1},\ j=1,\cdots,m-1 \\ r_{2n-2m+1}+\frac{1}{m}r_{2n-2m+1+j},\ j=1,\cdots,m-1 \\ c_{2n-2m+1}+\frac{1}{m}c_{2n-2m+1+j},\ j=1,\cdots,m-1}} \begin{pmatrix} C_{s_2\times s_2}(a_2) & \mathbf{0}_1 & O^{\mathsf{T}}_{t_2\times s_2} \\ \mathbf{0}_1^{\mathsf{T}} & -\frac{2m+1}{2m} & \mathbf{0}_2^{\mathsf{T}} \\ O_{t_2\times s_2} & \mathbf{0}_2 & F_{t_2\times t_2} \end{pmatrix},$$

where $s_2 = 2n - 2m$, $t_2 = m - 1$, $a_2 = 2 - \frac{1}{2m+1}$, $\mathbf{0}_1 = (0, \cdots, 0)^{\mathsf{T}}$ and $\mathbf{0}_2 = (0, \cdots, 0)^{\mathsf{T}}$ are s_2-dimensional column vector and t_2-dimensional column vector, respectively. By (A.11) and (A.12), we get

$$\left|\det(\mathcal{A}_{\bar{S}})\right| = \left(\frac{4n}{3} + \frac{2m}{3} + \frac{1}{6}\right) \times \left(\frac{3}{4}\right)^{n-m-1} \times \left(\frac{1}{2}\right)^{m-1}.$$

(3). If $\#S = m$ and $2n \in S,\ n \notin S$, by elementary transformation that exchanges any two rows and corresponding two columns, the original matrix $\mathcal{A}_{\bar{S}}$ can be transformed into (A.8), where $s = 2n - 2m + 2$, $t = m - 2$, $a = \frac{3}{2}$. Again using elementary transformations, we have

$$\begin{pmatrix} C_{s\times s}(a) & E^{\mathsf{T}}_{t\times s} \\ E_{t\times s} & D_{t\times t} \end{pmatrix} \xlongequal[\substack{r_{2n-2m+2}+\frac{1}{m-1}r_{2n-2m+2+j},\ j=1,\cdots,m-2 \\ c_{2n-2m+2}+\frac{1}{m-1}c_{2n-2m+2+j},\ j=1,\cdots,m-2}]{\substack{r_{2n-2m+2+j}-r_{2n-2m+2},\ j=1,\cdots,m-2 \\ c_{2n-2m+2+j}-c_{2n-2m+2},\ j=1,\cdots,m-2}} \begin{pmatrix} C_{s_3\times s_3}(a_3) & O^{\mathsf{T}}_{t_3\times s_3} \\ O_{t_3\times s_3} & F_{t_3\times t_3} \end{pmatrix}.$$

where $s_3 = 2n - 2m + 2$, $t_3 = m - 2$, $a_3 = 2 - \frac{1}{2(m-1)}$. By (A.11) and (A.12), we have

$$\left|\det\left(\mathcal{A}_{\bar{S}}\right)\right| = \left|\frac{4n}{3} + \frac{2m}{3} - \frac{3}{2}\right| \times \left(\frac{3}{4}\right)^{n-m} \times \left(\frac{1}{2}\right)^{m-2}.$$

(4). If $\#S = m$ and $n \in S,\ 2n \notin S$, by elementary transformation that exchanges any two rows and corresponding two columns, the original matrix $\mathcal{A}_{\bar{S}}$ can be transformed into (A.8), where $s = 2n - 2m + 1$, $t = m - 1$, $a = 1$. Again using elementary transformations, we have

$$\begin{pmatrix} C_{s\times s}(a) & E^{\mathsf{T}}_{t\times s} \\ E_{t\times s} & D_{t\times t} \end{pmatrix} \xrightarrow[\substack{r_{2n-2m+2}-r_{2n-2m+1},\ c_{2n-2m+2}-c_{2n-2m+1} \\ r_{2n-2m+1}+\frac{2m-2}{2m-1}r_{2n-2m+2},\ c_{2n-2m+1}+\frac{2m-2}{2m-1}c_{2n-2m+2}}]{\substack{r_{2n-2m+2+j}-r_{2n-2m+2},\ j=1,\cdots,m-2 \\ c_{2n-2m+2+j}-c_{2n-2m+2},\ j=1,\cdots,m-2 \\ r_{2n-2m+2}+\frac{1}{m-1}r_{2n-2m+2+j},\ j=1,\cdots,m-2 \\ c_{2n-2m+2}+\frac{1}{m-1}c_{2n-2m+2+j},\ j=1,\cdots,m-2}} \begin{pmatrix} C_{s_4\times s_4}(a_4) & \mathbf{0}_1 & O^{\mathsf{T}}_{t_4\times s_4} \\ \mathbf{0}_1^{\mathsf{T}} & -\frac{2m-1}{2m-2} & \mathbf{0}_2^{\mathsf{T}} \\ O_{t_4\times s_4} & \mathbf{0}_2 & F_{t_4\times t_4} \end{pmatrix},$$

where $s_4 = 2n - 2m + 1$, $t_4 = m - 2$, $a_4 = 2 - \frac{1}{2m-1}$, $\mathbf{0}_1 = (0, \cdots, 0)^{\mathsf{T}}$ and $\mathbf{0}_2 = (0, \cdots, 0)^{\mathsf{T}}$ are s_4-dimensional column vector and t_4-dimensional column vector, respectively. By (A.11) and (A.12), we have

$$\left|\det\left(\mathcal{A}_{\bar{S}}\right)\right| = \left|\frac{4n}{3} + \frac{2m}{3} - \frac{3}{2}\right| \times \left(\frac{3}{4}\right)^{n-m} \times \left(\frac{1}{2}\right)^{m-2}.$$

2. When $N = 2n + 1$, by (A.11) and (A.12) we have

$$\left|\det\left(\mathcal{A}_{\bar{S}}\right)\right| = \begin{cases} \left|\frac{4n}{3} + \frac{2m}{3} - \frac{7}{6}\right| \times \left(\frac{3}{4}\right)^{n-m+1} \times \left(\frac{1}{2}\right)^{m-2}, & \text{for } \#S = m \text{ and } 2n+1 \in S, \\ \left|\frac{4n}{3} + \frac{2m}{3} + \frac{1}{2}\right| \times \left(\frac{3}{4}\right)^{n-m} \times \left(\frac{1}{2}\right)^{m-1}, & \text{for } \#S = m \text{ and } 2n+1 \notin S. \end{cases}$$

Appendix B. Scaling of the Three-Component Gierer–Meinhardt Model

For completeness, we briefly discuss the rescaling of the original Gierer–Meinhardt model used to arrive at the form (1.3) considered in this paper. The majority of what follows is a reproduction of the brief discussion in the introduction of Iron et al. (2001); we perform here an additional rescaling to include the third component w.

The original Gierer–Meinhardt model of Gierer and Meinhardt (1972) is

$$\begin{cases} u_t = D_u u_{xx} - \mu_u u + c_u \rho \dfrac{u^r}{v^s} + \sigma_u \rho & \\ & x \in (-\ell, \ell), \quad t \geq 0, \\ v_t = D_v v_{xx} - \mu_v v + c_v \rho \dfrac{u^p}{v^q} & \\ \text{Neumann boundary conditions for at } x = \pm 1. & \end{cases} \tag{B.1}$$

where u and v are the concentration of the activator and the inhibitor; D_u and D_v are the diffusion coefficients for the activator and inhibitor, respectively, with D_u small; ρ is the rate of production of the activator and inhibitor, μ_u and μ_v are the decay rates of the activator and inhibitor, σ_u is the source term for the activator, which is small. We consider the simplest case when $r = 2$, $s = 1$, $p = 2$, $q = 0$ and add an inhibitor w, which acts as a feedback regulator that influences the production rate of the activator or inhibitor based on the current state of the system, providing a feedback loop. Then we have the following extended system:

$$\begin{cases} u_t = D_u u_{xx} - \mu_u u + c_u \rho \dfrac{u^2}{v} + \sigma_u \rho - kw \\ v_t = D_v v_{xx} - \mu_v v + c_v \rho u^2 \\ w_t = D_w w_{xx} + c_w u - \mu_w w \\ \text{Neumann boundary conditions for at } x = \pm\ell. \end{cases} \quad x \in (-\ell, \ell), \quad t \geq 0, \tag{B.2}$$

Since D_u and σ_u are assumed to be small in Gierer and Meinhardt (1972), we denote $D_u = (\mu_u + k)\varepsilon^2 \ll 1$ and $\sigma_u \rho = \frac{(\mu_u+k)^2}{c_u \rho} \sigma \varepsilon^2 \ll 1$. Following Iron et al. (2001), we let

$$u = \frac{(\mu_u + k)\tilde{u}}{\varepsilon c_u \rho}, \; v = \frac{\tilde{v}}{\varepsilon}, \; w = \frac{(\mu_u + k)\tilde{w}}{\varepsilon c_u \rho}, \; \tilde{t} = (\mu_u + k)t, \; h = \frac{c_v}{\mu_v} \frac{(\mu_u + k)^2}{c_u^2 \rho}$$
$$\tilde{D}_v = \frac{D_v}{\tilde{\mu}_v}, \; \tilde{D}_w = \frac{D_w}{\tilde{\mu}_w}, \; \tau_v = \frac{(\mu_u + k)}{\mu_v}, \; \tau_w = \frac{(\mu_u + k)}{\mu_w}, \; \kappa = \frac{k}{(\mu_u + k)}, \; c = \frac{c_w}{\mu_w}. \tag{B.3}$$

Then

$$\begin{cases} \tilde{u}_{\tilde{t}} = \varepsilon^2 \tilde{u}_{xx} - (1 - \kappa)\tilde{u} + \dfrac{\tilde{u}^2}{\tilde{v}} + \sigma \rho \varepsilon^3 - \kappa \tilde{w} \\ \tau_v \tilde{v}_{\tilde{t}} = \tilde{D}_v \tilde{v}_{xx} - \tilde{v} + h \dfrac{\tilde{u}^2}{\varepsilon} \\ \tau_w \tilde{w}_{\tilde{t}} = \tilde{D}_w \tilde{w}_{xx} + c\tilde{u} - \tilde{w} \\ \text{Neumann boundary conditions for at } x = \pm\ell. \end{cases} \quad x \in (-\ell, \ell), \quad t \geq 0, \tag{B.4}$$

Neglecting the higher order constant $\sigma \rho \varepsilon^3$ and dropping the tilde, we obtain

$$\begin{cases} u_t = \varepsilon^2 u_{xx} - (1 - \kappa)u + \dfrac{u^2}{v} - \kappa w \\ \tau_v v_t = D_v v_{xx} - v + h \dfrac{u^2}{\varepsilon} \\ \tau_w w_t = D_w w_{xx} + cu - w \\ \text{Neumann boundary conditions for at } x = \pm\ell. \end{cases} \quad x \in (-\ell, \ell), \quad t \geq 0, \tag{B.5}$$

Finally, Setting $h = 1, c = 1$ and $\tau_v = 0, \; D_w = 0$ gives us the rescaled system (1.1). We remark that taking $\tau_v = 0, \; D_w = 0$ leads to a singular reduction of the system since it alters the order of the differential equation. The generalizability of the conclusions drawn in this paper to the case where τ_v and D_w are small but not zero remains uncertain.

Acknowledgements S.Q. Xie acknowledges the support from Hunan Natural Science Foundation under Grant Number 2023JJ40111, as well as the funding from the Changsha Natural Science Foundation, Grant Number KQ2208006. W. Yang is partially supported by National Key R&D Program of China 2022YFA1006800, NSFC No. 12171456, No. 12271369 and SRG2023-00067-FST.

References

Al Saadi, F., Gai, C., Nelson, M.: Localized pattern formation: semi-strong interaction asymptotic analysis for three components model. Proc. R. Soc. A **480**(2281), 20230591 (2024)

Bastiaansen, R., Doelman, A.: The dynamics of disappearing pulses in a singularly perturbed reaction-diffusion system with parameters that vary in time and space. Phys. D Nonlinear Phenom. **388**, 45–72 (2019)

Chen, W., Ward, M.J.: Oscillatory instabilities and dynamics of multi-spike patterns for the one-dimensional Gray-Scott model. Eur. J. Appl. Math. **20**(2), 187–214 (2009)

Chen, W., Ward, M.J.: The stability and dynamics of localized spot patterns in the two-dimensional Gray-Scott model. SIAM J. Appl. Dyn. Syst. **10**(2), 582–666 (2011)

Chirilus-Bruckner, M., van Heijster, P., Ikeda, H., Rademacher, J.D.: Unfolding symmetric bogdanov-takens bifurcations for front dynamics in a reaction-diffusion system. J. Nonlinear Sci. **29**, 2911–2953 (2019)

Doelman, A., Gardner, R.A., Kaper, T.J.: A stability index analysis of 1-D patterns of the Gray-Scott model. Memoirs of the American Mathematical Society (2002)

Doelman, A., Kaper, T.J., Zegeling, P.A.: Pattern formation in the one-dimensional Gray-Scott model. Nonlinearity **10**(2), 523–563 (1997)

Doelman, A., Gardner, R.A., Kaper, T.J.: Large stable pulse solutions in reaction-diffusion equations. Indiana Univ. Math. J. **50**(1), 443–507 (2001)

Doelman, A., Kaper, T.J., van der Ploeg, H.: Spatially periodic and aperiodic multi-pulse patterns in the one-dimensional Gierer-Meinhardt equation. Methods Appl. Anal. **8**(3), 387–414 (2001)

Gierer, A., Meinhardt, H.: A theory of biological pattern formation. Kybernetik **12**(1), 30–39 (1972)

Giunta, V., Lombardo, M.C., Sammartino, M.: Pattern formation and transition to chaos in a chemotaxis model of acute inflammation. SIAM J. Appl. Dyn. Syst. **20**(4), 1844–1881 (2021)

Gomez, D., Mei, L., Wei, J.: Stable and unstable periodic spiky solutions for the Gray-Scott system and the Schnakenberg system. J. Dyn. Differ. Equ. **32**(1), 441–481 (2020)

Gomez, D., Mei, L., Wei, J.: Hopf bifurcation from spike solutions for the weak coupling Gierer-Meinhardt system. Eur. J. Appl. Math. **32**(1), 113–145 (2021)

Gurevich, S., Friedrich, R.: Moving and breathing localized structures in reaction-diffusion systems. Math. Model. Nat. Phenom. **8**(5), 84–94 (2013)

Gurevich, S., Amiranashvili, S., Purwins, H.-G.: Breathing dissipative solitons in three-component reaction-diffusion system. Phys. Rev. E **74**(6), 066201 (2006)

Iron, D., Ward, M.J.: The dynamics of multispike solutions to the one-dimensional Gierer-Meinhardt model. SIAM J. Appl. Math. **62**(6), 1924–1951 (2002)

Iron, D., Ward, M.J., Wei, J.: The stability of spike solutions to the one-dimensional Gierer-Meinhardt model. Phys. D Nonlinear Phenom. **150**(1–2), 25–62 (2001)

Iron, D., Wei, J., Winter, M.: Stability analysis of Turing patterns generated by the Schnakenberg model. J. Math. Biol. **49**(4), 358–390 (2004)

Kolokolnikov, T., Ward, M.J., Wei, J.: The existence and stability of spike equilibria in the one-dimensional Gray-Scott model: the low feed-rate regime. Stud. Appl. Math. **115**(1), 21–71 (2005)

Kolokolnikov, T., Ward, M.J., Wei, J.: The existence and stability of spike equilibria in the one-dimensional Gray-Scott model: the pulse-splitting regime. Phys. D Nonlinear Phenom. **202**(3–4), 258–293 (2005)

Kolokolnikov, T., Ward, M.J., Wei, J.: Slow translational instabilities of spike patterns in the one-dimensional Gray-Scott model. Interfaces Free Boundaries **8**(2), 185–222 (2006)

Kolokolnikov, T., Paquin-Lefebvre, F., Ward, M.J.: Competition instabilities of spike patterns for the 1D Gierer-Meinhardt and Schnakenberg models are subcritical. Nonlinearity **34**(1), 273–312 (2021)

Or-Guil, M., Bode, M., Schenk, C., Purwins, H.-G.: Spot bifurcations in three-component reaction-diffusion systems: the onset of propagation. Phys. Rev. E **57**(6), 6432–6437 (1998)

Pearson, J.E.: Complex patterns in a simple system. Science **261**(5118), 189–192 (1993)

P. S. Inc., “Flexpde 7,” https://www.pdesolutions.com/index.html, 2020

Schnakenberg, J.: Simple chemical reaction systems with limit cycle behaviour. J. Theor. Biol. **81**(3), 389–400 (1979)

Tzou, J., Xie, S.: Oscillatory translational instabilities of spot patterns in the schnakenberg system on general 2d domains. Nonlinearity **36**(5), 2473 (2023)
Vanag, V.K., Epstein, I.R.: Localized patterns in reaction-diffusion systems. Chaos Interdiscip. J. Nonlinear Sci. **17**(3), 037110 (2007)
Veerman, F.: Breathing pulses in singularly perturbed reaction-diffusion systems. Nonlinearity **28**(7), 2211–2246 (2015)
Ward, M.J., Wei, J.: The existence and stability of asymmetric spike patterns for the Schnakenberg model. Stud. Appl. Math. **109**(3), 229–264 (2002)
Ward, M.J., Wei, J.: Hopf bifurcation of spike solutions for the shadow Gierer-Meinhardt model. Eur. J. Appl. Math. **14**(6), 677–711 (2003)
Ward, M.J., Wei, J.: Hopf bifurcations and oscillatory instabilities of spike solutions for the one-dimensional Gierer-Meinhardt model. J. Nonlinear Sci. **13**(2), 209–264 (2003)
Wei, J., Winter, M.: Mathematical Aspects of Pattern Formation in Biological Systems, vol. 189. Springer Science & Business Media (2013)
Wei, J., Winter, M.: Stable spike clusters for the one-dimensional Gierer-Meinhardt system. Eur. J. Appl. Math. **28**(4), 576–635 (2017)
Wei, J., Winter, M., Yang, W.: Stable spike clusters for the precursor Gierer-Meinhardt system in $\mathbb{R}^2$. Calc. Var. Partial Differ. Equ. **56**(5), 142 (2017)
Xie, S., Kolokolnikov, T.: Moving and jumping spot in a two-dimensional reaction-diffusion model. Nonlinearity **30**(4), 1536–1563 (2017)
Xie, S., Kolokolnikov, T., Nishiura, Y.: Complex oscillatory motion of multiple spikes in a three-component Schnakenberg system. Nonlinearity **34**(8), 5708–5743 (2021)